Chapter 10
Energy Management Systems for Intelligent Buildings in Smart Grids

Alessandra Parisio, Marco Molinari, Damiano Varagnolo and Karl H. Johansson

10.1 Introduction

It is well-known that buildings contribute a large portion of the overall energy use worldwide. Buildings need to be more sustainable and environmentally friendly and the role of buildings in the next-generation energy grids has to be rethought. In fact, as shown in Fig. 10.1, *smart* buildings should be designed to integrate not just loads but also distributed generation (e.g., storage systems and renewable energy resources); to sense, compute, communicate, and actuate; to purchase, generate, and sell power to and from its energy suppliers; to take advantage of local generation to implement

This work is supported by the Swedish Foundation for Strategic Research (SSF), the Swedish Research Council (VR), and the Knut and Alice Wallenberg Foundation (KAW), the Swedish Governmental Agency for Innovation Systems (VINNOVA), the Celtic Plus project SENDATE-Extend (C2015/3-3), the Swedish research council Norrbottens Forskningsråd project DISTRACT, and the Swedish Energimyndigheten E2B2 project Green Power.

A. Parisio (✉)
School of Electrical and Electronic Engineering, The University of Manchester, Ferranti Building-C5, Manchester M13 9PL, UK
e-mail: alessandra.parisio@manchester.ac.uk

M. Molinari
School of Electrical Engineering, KTH Royal Institute of Technology, 100 44 Stockholm, Sweden
e-mail: marcomo@kth.se

D. Varagnolo
Department of Computer Science, Electrical and Space Engineering, Luleå University of Technology, Forskargatan 1, 971 87 Luleå, Sweden
e-mail: damiano.varagnolo@ltu.se

K.H. Johansson
ACCESS Linnaeus Centre, School of Electrical Engineering, KTH Royal Institute of Technology, 100 44 Stockholm, Sweden
e-mail: kallej@kth.se

J.T. Wen and S. Mishra (eds.), *Intelligent Building Control Systems*, Advances in Industrial Control, https://doi.org/10.1007/978-3-319-68462-8_10

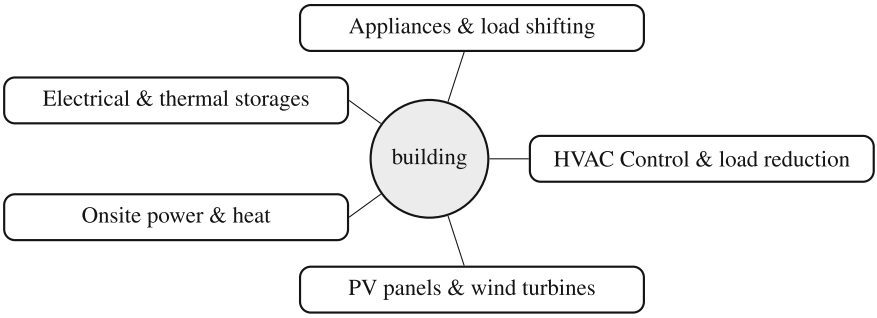

Fig. 10.1 Technologies that can enable building-to-grid integration

demand response and optimize the energy usage. Loads of a smart building can be divided either into non-flexible ...or flexible (instead of schedulable) (critical) or schedulable loads, which implies that the decision-making algorithms should aim not only to lower the energy use without sacrificing the comfort of the occupants, but also try to support the network operator and reduce the overall environmental impact.

Hence, designing Energy Management Systems (EMS) for achieving sustainable building operation requires that several challenges are addressed. The EMS must be able to deal with the complexity such as conflicting objectives, decision-making and coordination of decisions distributed over multiple units. The increased Information and Communication Technology (ICT) capabilities can enable a wider, more sophisticated range of intelligent methods and innovative schemes to facilitate the management of energy demand and generation, including demand response, smart appliances, and price and carbon-based signals.

An EMS for smart building will: (1) respond to signals from the grid and take action on this basis (e.g., decreasing energy use when prices are high or automatically shifting consumption to times when prices are lower); (2) manage local generation facilities, such as solar panels, and feedback into the grid any energy; (3) optimally schedule storage devices, which can be used to balance out the smart grid and respond to price signals to help decrease the electricity bills [1].

Besides, this EMS needs to incorporate users into the design (to be responsive to occupants and improve their comfort) and to take advantage of the flexibility opportunities offered by storage devices (to counteract the intermittent behavior of renewable generation by providing ancillary services). These functionalities could

represent new business case opportunities for various market actors such as aggregators, energy service companies, and network operators. An advanced EMS should not come with tailored configurations, but rather be cost-effective in order to be deployed by a wide range of consumers.

Such an innovative and advanced EMS would make buildings smart and smart buildings are an essential element of smart grids. Although advanced control and automation systems are becoming quite widespread, standardized and holistic solutions are still not available [1].

In this chapter, we describe the design of and scheduling frameworks for optimal management of smart buildings. In Sect. 10.2 we illustrate novel stochastic MPC schemes for HVAC systems and discuss their performance along with practical implementation issues. In Sect. 10.3, we illustrate how to integrate local generation capabilities and storage systems into a holistic building energy management framework. In Sect. 10.4, we briefly describe three demonstrators located in Sweden and UK that support ongoing research activities and experiments on an EMS for smart buildings. In Sect. 10.5, we show that data centers can play several different schemes typical of residential smart buildings data centers and they can act as bridges between three types of networks: electrical, thermal and information networks. Finally, in Sect. 10.6 we draw some conclusions.

10.2 Control of HVAC Systems via Scenario-Based Implicit and Explicit MPC

In this section, we discuss the design and the implementation of stochastic MPC approaches for the effective control of HVAC systems. HVAC systems are employed to maintain acceptable thermal comfort and CO_2 levels in buildings. A relevant share of the overall energy use in buildings is for ventilation, space heating and cooling; effective control of building HVAC, used to maintain acceptable thermal comfort and indoor air quality, is seen as an attractive approach to cost-efficiently decrease the energy use and increase the sustainability in the built environment, and has been the object of relevant research effort in recent years [2]. An improved building management can potentially lead to energy savings estimated between 5 and 30% of the total energy use [3, 4]. HVAC control systems performance can be improved by using predictive strategies.

In particular, MPC schemes are expected to become a common solution for buildings in a few years because of their capability to incorporate time-dependent energy costs, bounds on the control actions, comfort requirements, and account for uncertainties, e.g., in the models and in the forecasts [5–7]. Successful implementations will likely be based on stochastic MPC schemes with probabilistic constraints since indoor air conditions are intrinsically affected by stochastic disturbances, e.g., weather conditions and occupancy levels.

In this section, we propose MPC formulations that take into account uncertainties in the weather predictions and occupancy levels, and adopt the scenario-based distribution-free approach described in [8]. This approach does not require to assume Gaussian disturbances, as commonly done in the literature. This assumption makes the problems easier to solve, but it is often an invalid assumption in practical situations, especially for solar radiation and occupancy processes.

To address all the issues above and yet obtain an effective and computationally tractable MPC problem, we propose a stochastic MPC (SMPC) scheme that comprises two linear stochastic MPC problems and a dynamical approach for learning the statistics of the uncertainties. This SMPC scheme aims at controlling both indoor temperature and CO_2 concentration levels and is described in more detail in Sect. 10.2.3. The control action is computed by considering a given number of uncertainty samples and does not require any a-priori assumptions on the distributions of the uncertain variables. This implicit MPC formulation and its experimental evaluation are then discussed in Sect. 10.2.4.

The drawback associated with the proposed implicit MPC scheme is its online computational burden, whose implementation on cheap hardware platforms (such as in Programmable Logic Controllers (PLCs)) and integration in Building Automation Systems (BASs) may become prohibitive. In addition, scenario-based approaches require generation of a large number of scenarios online, further increasing the computational burden. A possible solution is to determine off-line the explicit solution of the MPC problem as a function of the current building state. This leads to explicit solutions from multiparametric programs [9, 10] where the state vector is treated as a vector of parameters, so that the optimal control profile becomes a Piecewise Affine (PWA) function of the initial state. In this way, the computational requirements of the MPC scheme reduce to a function evaluation problem, which can be implemented using simple software and cheap hardware. We formulate and describe such an explicit MPC scheme for controlling the HVAC system in Sect. 10.2.5.

Before presenting both our implicit and explicit MPC schemes, we review the relevant literature in Sect. 10.2.1. Various physical and control-oriented models of the thermal and CO_2 concentration dynamics are then described in Sect. 10.2.2. For further details, we refer the interested reader to [11–13] and point out that, even if we focus on one single room or thermal zone, extensions to whole building enclosures or to room networks are possible since the overall building energy use can be computed as the sum the energy usages of individual thermal zones [14].

10.2.1 Review of Control Strategies for HVAC Systems

HVAC control has been extensively explored by both researchers and practitioners. Typical practice does not require coordination between HVAC control and blinds and lighting control; nonetheless, it has been experimentally shown that coordination may lead to significant energetic benefits [15].

The HVAC control problem is usually divided into a hierarchical cascade of two problems: *HVAC scheduling* and *HVAC regulation* (see [16] and references therein). More precisely,

scheduling means deciding both when and in which mode to operate the various HVAC subsystems (e.g., on or off), and which values should be assigned to the setpoints of subsystems (e.g., the temperature and CO_2 levels of thermal zones);

regulation means rejecting disturbances so that the actual conditions in the built environment follow closely the setpoints specified by the scheduling algorithm.

The regulation part is usually performed by means of low-level Proportional-Integral Derivative (PID) controllers, which generally provide satisfactory tracking performance, mainly because temperature and CO_2 dynamics are slow (see, for example, [13], where experimental evidence shows that temperature and CO_2 concentration have time constants of minutes in a laboratory of approximately 80 m^2).

The scheduling part is interesting from research perspectives, and is where the state of the art and the common practice differ. We can categorize the existing strategies as follows:

rule-based strategies: the control inputs are computed through rules of the type "if *condition* then *action*" where the *condition* statement typically involves thresholds and other numerical values that play the role of control parameters. Rule-based strategies may be (see also [15] and references therein):

- *open-loop,* which do not make use of information to change the scheduling outcomes;
- *reactive,* which use information on the current and past states of the system to change the scheduling outcomes;
- *predictive,* which change the scheduling outcomes if forecasts of building usage change.

Predictive approaches are the most powerful ones; their main drawback is that they are associated to a larger set of rules and parameters, and this increases the difficulty in tuning [15];

model-based predictive strategies: the control strategy is determined by combining an opportune model of the building with forecasts of the disturbances to facilitate a search for the input steering the forecast system trajectory to minimize a certain objective function. This category may be divided into:

- *control-oriented strategies,* where modeling of the dynamics is typically a gray- or black-box model, potentially trained using some system identification procedure;
- *machine-learning-oriented strategies,* where models are typically non-parametric and data-driven (e.g., learned through opportune neural networks).

We notice that evaluations of model-based predictive strategies in smart buildings consistently show increased performance with respect to non-predictive control strategies [7, 17]. The current trend seems to add to these predictive strategies robustness with respect to uncertainties in the forecasts [18, 19].

10.2.2 HVAC System Modeling

The model used in this chapter is derived by using thermodynamics laws with a thermal network approach, as described in Sect. 10.2.2.1. Compared to data-driven approaches, this approach provides a clear physical interpretation and features greater modeling generality, allowing thus a straightforward adjustment to other buildings.

Unfortunately, physical-based equations describing indoor CO_2 and temperature dynamics include nonlinearities. Posing then the problem of minimizing the energy use while keeping both indoor CO_2 and thermal comfort as one single problem results in a non-convex problem, and this would eventually lead to problems at the implementation stage. In Sect. 10.2.2.2, we thus address this issue by first deriving control-oriented models of both the CO_2 and thermal dynamics, and then formulating the overall HVAC control problem as a cascade of two linear (and thus more easily implementable) problems.

10.2.2.1 Physical Modeling of HVAC Systems

To model the energy flows in a thermal zone, we consider the flows through its envelope (i.e., walls and windows), the flows generated within the zone (e.g., occupants, lights, and equipment), and the flows provided by the heating and cooling systems via the ventilation and the heating emission systems. Our main assumptions are then that:

- there are no air latent heat, e.g., from vapor production, is neglected infiltrations, so that the inlet airflow in the zone equals the outlet airflow;
- the air in the zone is well mixed;
- latent heat, e.g., from vapor production, is neglected;
- there are no thermal bridges.

Given the assumptions above, the dynamics of the room temperature can be calculated by computing the energy balance equations of the zone, the latter modeled as a lumped node, i.e.,

$$m_{\text{air,zone}} c_{\text{pa}} \frac{dT_{\text{room}}}{dt} = Q_{\text{venting}} + Q_{\text{int}} + \sum_{\text{j}} Q_{\text{wall,j}} + \sum_{j} Q_{\text{win,j}} + Q_{\text{heating}} + Q_{\text{cooling}}. \tag{10.1}$$

In (10.1), the left-hand side represents the heat stored in the air of the zone, Q_{venting} is the heat flow due to ventilation, Q_{int} are the internal gains (the sum of the heat flows due to occupancy, equipment, and lighting), $Q_{\text{wall,j}}$ and $Q_{\text{win,j}}$ represent the heat flows exchanged between walls and room and windows and room, respectively, Q_{cooling} and Q_{heating} are the cooling and heating flows necessary to keep the within thermally comfortable conditions.

The explicit dependence between room the variation of the temperature T_{room} and the heat flows is then obtained by manipulating (10.1):

$$\begin{aligned}\frac{dT_{\text{room}}}{dt} = \frac{\dot{m}_{\text{venting}}\Delta T_{\text{venting}}}{m_{\text{air,zone}}} + \sum_j \frac{h_i A^j_{\text{wall}}\left(T^j_{\text{wall,i}} - T_{\text{room}}\right)}{m_{\text{air,zone}}c_{\text{pa}}} \\ + \sum_j \frac{\left(T_{\text{amb}} - T_{\text{room}}\right)}{R^j_{\text{win}} m_{\text{air,zone}}c_{\text{pa}}} + \frac{cN_s}{m_{\text{air,zone}}c_{\text{pa}}} \\ + \frac{\sum_j G^j A^j_{\text{win}} I^j}{m_{\text{air,zone}}c_{\text{pa}}} + \frac{A_{\text{rad}}h_{\text{rad}}\Delta T_{\text{h,rad}}}{m_{\text{air,zone}}c_{\text{pa}}}\end{aligned} \tag{10.2}$$

where

$$\begin{aligned}Q_{\text{venting}} &= \dot{m}_{\text{venting}}c_{\text{pa}}\Delta T_{\text{venting}} = \dot{m}_{\text{venting}}c_{\text{pa}}\left(T_{\text{air,sa}} - T_{\text{room}}\right), \\ Q_{\text{int}} &= cN_{\text{people}}, \\ Q_{\text{heating}} &= A_{\text{rad}}h_{\text{rad}}\Delta T_{\text{h,rad}} = A_{\text{rad}}h_{\text{rad}}\left(T_{\text{mr}} - T_{\text{room}}\right).\end{aligned}$$

The parameters involved in (10.2) are described in Table 10.1, reported in the appendix and presenting the parameters in alphabetical order for reading convenience. The indoor wall temperature $T^{\text{j}}_{\text{wall,i}}$ in the j-th surface is calculated with a further energy balance on the outdoor wall surface and on the indoor wall surface, with walls modeled as three resistance and two capacitance (3R2C) systems [20, 21].

The air mass flow for ventilation $\dot{m}_{vent}$ in (10.2) is determined by the CO_2 concentration in the room, calculated after the model proposed in [22] as:

$$V\frac{dC_{\text{CO}_2}}{dt} = \left(\dot{m}_{vent}C_{\text{CO}_2,i} + g_{\text{CO}_2}N_{people}\right) - \dot{m}_{vent}C_{\text{CO}_2}. \tag{10.3}$$

The models above capture the main features of the dynamics of the temperature and CO_2 concentrations. Their constants determine then the physical characteristics of a generic room, and this allows a straightforward adaptation of the models to other rooms. For example, the surface of a heating emission system may be conveniently modeled with a parameter A_{rad} accounting for different sizes of the heating units. We notice that, however, heating systems with a relevant thermal mass, like floor heating, are characterized by delays that should not be neglected. In this case, the models should be adapted to account for ad-hoc time delays.

Table 10.1 Summary of the parameters involved in the building model

A_{rad}	$[m^2]$	Emission area of the radiators
A^j_{wall}	$[m^2]$	Wall area on the j-th surface
A^j_{win}	$[m^2]$	Area of the window on the j-th surface
c	$[W]$	Constant related to equipment and occupants activity
$C_{CO_{2,i}}$	[ppmV]	Inlet air CO_2concentration, assumed equal to outdoor CO_2 concentration
C_{CO_2}	[ppmV]	Concentration of CO_2 within the room
c_{pa}	$[J/kg°C]$	Specific heat of the dry air
g_{CO_2}	$[m^3_{CO_2}$/pers.]	Generation rate of CO_2 per person
G^j	$[-]$	G-value (SHGC) of the window on the j-th surface
h_{i}	$[W/\mathrm{m}^2°\mathrm{C}]$	Indoor heat transfer coefficient
h_{rad}	$[W/m^2°C]$	Heat transfer coefficient of the radiators
I^j	$[W/m^2]$	Solar radiation on the j-th surface
$m_{air,zone}$	$[kg]$	Air mass in the room
$\dot{m}_{vent}$	$[kg/s]$	Ventilation mass flow
N_{people}	$[-]$	Number of occupants in the room
R^j_{win}	$[°C/W]$	Thermal resistance of the window on the j-th surface
$T_{air,sa}$	$[°C]$	Supply air temperature
T_{amb}	$[°C]$	Outdoor temperature
T^j_i	$[°C]$	Indoor surface temperature of the wall on the j-th surface
T_mr	$[°C]$	Mean radiant temperature of the radiators
V	$[m^3]$	Volume of the air inside the room

10.2.2.2 Control-Oriented Modeling of HVAC systems

As mentioned above, we aim at rewriting the nonlinear equations. (10.2) and (10.3) as linear equations and at developing control-oriented models of both the CO_2 and thermal dynamics. We start by pointing out that: *(i)* the CO_2 concentration dynamics are independent of the thermal ones; *(ii)* CO_2 comfort has priority, entailing that the ventilation level cannot be lower than the one ensuring an acceptable CO_2 level in the room.

This allows us to address two separated subproblems: *(i)* the CO_2-SMPC problem, which aims at minimizing energy use while keeping CO_2 levels in given comfort bounds; *(ii)* the T-SMPC problem, controlling instead the indoor temperature and deciding the additional ventilation level guaranteeing the thermal comfort. The output of the sequence of the CO_2-SMPC problem is a sequence of air flow rates coming from the ventilation system over the whole prediction horizon, which is then integrated into the T-SMPC problem to account for the corresponding heat flow.

In the following, we present the control-oriented models incorporated into the CO_2-SMPC and T-SMPC problems.

Control-oriented model of the CO_2 concentration dynamics

The model state x_{CO_2} and the model output y_{CO_2} are equal to the nonnegative difference between the CO_2 concentration in the room and the inlet air CO_2 concentration (the latter one assumed to be equal to the outdoor CO_2 concentration levels). The model disturbance $w_{CO_2}(k)$ represents instead the number of occupants.

We derive an equivalent linear model of the CO_2 concentration dynamics by introducing the auxiliary input $u_{CO_2} := \dot{m}^{CO_2}_{venting} \cdot x_{CO_2}$ representing the reduction in the indoor CO_2 concentration levels induced by $\dot{m}^{CO_2}_{venting}$. To satisfy the physical bounds on the original control input $\dot{m}^{CO_2}_{venting}$, we introduce the following additional constraints on the auxiliary input u_{CO_2},

$$\dot{m}^{min}_{venting} \cdot x_{CO_2}(k) \leq u_{CO_2}(k) \leq \dot{m}^{max}_{venting} \cdot x_{CO_2}(k). \tag{10.4}$$

The CO_2 concentration dynamics can eventually be described by the discrete-time Linear Time Invariant (LTI) system

$$\begin{aligned} x_{CO_2}(k+1) &= a x_{CO_2}(k) + b u_{CO_2}(k) + e w_{CO_2}(k) \\ y_{CO_2}(k) &= x_{CO_2}(k). \end{aligned} \tag{10.5}$$

Control-oriented model of the thermal dynamics

The state of the model is the vector of the temperatures of the room, walls, floor, and ceiling. The model disturbances represent the outdoor temperature, the incident solar radiation, the internal gains, and the heat flows due to occupancy, equipments, and lighting. The control inputs required to actuate the HVAC system are the temperature of the supplied air, T_{sa}, the mean radiant temperature of the radiators, T_{mr}, and the additional air flow rate required for guaranteeing the thermal comfort, $\Delta\dot{m}_{venting}$, defined as $\Delta\dot{m}_{venting} := \dot{m}_{venting} - \dot{m}^{CO_2}_{venting}$.

We derive an equivalent linear model of the thermal dynamics by introducing the nonnegative variables ΔT_h, ΔT_c, Δu_h and Δu_c as auxiliary inputs s.t.

$$\begin{aligned} \Delta T_h - \Delta T_c &:= T_{sa} - T_{room} \\ \Delta T_h + \Delta T_c &:= \left| T_{sa} - T_{room} \right| \\ \Delta u_h - \Delta u_c &:= \Delta\dot{m}_{venting}\left(T_{sa} - T_{room}\right) \\ \Delta u_h + \Delta u_c &:= \Delta\dot{m}_{venting}\left| T_{sa} - T_{room} \right|. \end{aligned}$$

By introducing the auxiliary inputs above, the heat flows in (10.2) can be rewritten as

$$\begin{aligned} Q_{venting} &= \dot{m}^{CO_2}_{venting} c_{pa}\left(\Delta T_h - \Delta T_c\right) + c_{pa}\left(\Delta u_h - \Delta u_c\right) \\ Q_{heating} &= A_{rad} h_{rad} \Delta T_{h,rad}. \end{aligned}$$

We consider the following additional constraints to meet physical bounds on the original control inputs

$$\begin{aligned} 0 &\leq \Delta T_{\mathrm{h}}(k) \leq T_{\mathrm{sa}}^{\max} - T_{\mathrm{room}}(k) \\ 0 &\leq \Delta T_{\mathrm{c}}(k) \leq T_{\mathrm{room}}(k) - T_{\mathrm{sa}}^{\min} \end{aligned} \tag{10.6}$$

$$\begin{aligned} 0 &\leq \Delta u_{\mathrm{h}}(k) \leq \Delta \dot{m}_{\mathrm{venting}}^{\max}(k) \Delta T_{\mathrm{h}}(k) \\ 0 &\leq \Delta u_{\mathrm{c}}(k) \leq \Delta \dot{m}_{\mathrm{venting}}^{\max}(k) \Delta T_{\mathrm{c}}(k). \end{aligned} \tag{10.7}$$

where $\Delta \dot{m}_{\mathrm{venting}}^{\max}(k) := \dot{m}_{\mathrm{venting}}^{\max} - \dot{m}_{\mathrm{venting}}^{\mathrm{CO_2}}(k)$. Constraints (10.6) and (10.7) rule out the possibility of simultaneous heating and cooling modes, which can happen when T_{room} is greater than $T_{\mathrm{sa}}^{\min}$ or smaller that $T_{\mathrm{sa}}^{\max}$ or when it is convenient to require a stronger but unfeasible cooling/heating action. Bounds on T_{sa} have to be carefully defined and the physical bounds on the supply air temperature should be considered.

With the newly introduced variables, the dynamics of the indoor temperature can be modeled with the discrete-time LTI system

$$\begin{aligned} x_{\mathrm{T}}(k+1) &= A_{\mathrm{T}} x_{\mathrm{T}}(k) + B_{\mathrm{T}}(k) u_{\mathrm{T}}(k) + E_{\mathrm{T}} w_{\mathrm{T}}(k) \\ y_{\mathrm{T}}(k) &= C_{\mathrm{T}} x_{\mathrm{T}}(k), \end{aligned} \tag{10.8}$$

where the state $x_{\mathrm{T}}(k)$ contains the temperatures of the room and of the inner and outer parts of the walls, $u_{\mathrm{T}}(k)$ is the input vector, as defined above, and $w_{\mathrm{T}}(k)$ is the vector of random disturbances (outdoor temperature, solar radiation, and internal heat gains). The output $y_{\mathrm{T}}(k)$ is the indoor temperature at time k. We notice that the input matrix $B_{\mathrm{T}}(k)$ is time-varying since it depends on $\dot{m}_{\mathrm{venting}}^{\mathrm{CO_2}}(k)$.

10.2.3 SMPC Problem Formulation for HVAC Systems

In Sect. 10.2.3.1, we formulate the stochastic MPC problem for optimizing HVAC operation and illustrate how a scenario-based approximation can be derived in Sect. 10.2.3.2.

10.2.3.1 Chance-Constrained MPC formulation

We start considering a generic discrete-time LTI systems with uncertainty of the form

$$\begin{aligned} x(k+1) &= Ax(k) + B(k)u(k) + Ew(k) \\ y(k) &= Cx(k), \end{aligned} \tag{10.9}$$

where $x(k) \in \mathcal{R}^n$ is the state, $u(k) \in \mathcal{R}^m$ is the control input, $w(k) \in \mathcal{R}^r$ is the stochastic disturbance and $y(k) \in \mathcal{R}^p$ is the output. Notice that, depending on

the controller under consideration (CO_2-SMPC or T-SMPC), (10.9) can represent either (10.5) or (10.8).

We define $\boldsymbol{x} := \left[x(1)^{\mathrm{T}}, \ldots, x(N)^{\mathrm{T}}\right]^{\mathrm{T}}$ the vector representing the state evolution over the prediction horizon N. Similarly, we define $\boldsymbol{u}$, $\boldsymbol{y}$ and $\boldsymbol{w}$. Prediction dynamics matrices $\boldsymbol{C}_A, \boldsymbol{C}_B, \boldsymbol{C}_E$ easily follow from (10.9) and the definitions of $\boldsymbol{x}$, $\boldsymbol{u}$, $\boldsymbol{y}$ and $\boldsymbol{w}$. Hence, we can express the output as a function of the initial state $x(0)$, i.e.,

$$\boldsymbol{y}^0 = \boldsymbol{C}_A x(0) + \boldsymbol{C}_B \boldsymbol{u} + \boldsymbol{C}_E \boldsymbol{w}, \tag{10.10}$$

with $x(0)$ the current measured value of the state.

Constraints (10.4) and (10.6) can be written in a compact form as mixed constraints on inputs and outputs. Using $\boldsymbol{y}^0$, we can write both comfort constraints and mixed constraints on inputs and outputs over the whole prediction horizon as $\boldsymbol{G}^u \boldsymbol{u} + \boldsymbol{G}^w \boldsymbol{w} \leq \boldsymbol{g}$, with the left-hand side being bi-affine functions in the vector of decision variables $\boldsymbol{u}$ and random variables $\boldsymbol{w}$, and $\boldsymbol{G}^u$, $\boldsymbol{G}^w$ and $\boldsymbol{g}$ being matrices of appropriate dimensions.

Constraints on inputs (e.g., (10.7) over the whole prediction horizon can be written as $\boldsymbol{F}\boldsymbol{u} \leq \boldsymbol{f}$, where $\boldsymbol{F}$ and $\boldsymbol{f}$ are matrices of appropriate dimensions.

To summarize, the linear constraints on the inputs and outputs (comfort constraints) over the prediction horizon are

$$\begin{aligned} \boldsymbol{G}^u \boldsymbol{u} + \boldsymbol{G}^w \boldsymbol{w} &\leq \boldsymbol{g} \\ \boldsymbol{F}\boldsymbol{u} &\leq \boldsymbol{f}. \end{aligned} \tag{10.11}$$

As introduced above, since it is possible to assume that these random constraints can be violated with a predefined probability $\alpha \in [0, 1]$, uncertainties can be handled by formulating the random constraints (10.11) as probabilistic constraints of the form

$$\mathbb{P}\left[\boldsymbol{G}^u \boldsymbol{u} + \boldsymbol{G}^w \boldsymbol{w} \leq \boldsymbol{g}\right] \geq 1 - \alpha.$$

To formulate the chance-constrained MPC problem we define a linear cost function over the whole prediction horizon as $J(x(0), \boldsymbol{u}) = \sum_{k=0}^{N-1} J(u(k))$. The control problem is formally stated as

$$\begin{aligned} \min_{\boldsymbol{u}} \quad & J(x(0), \boldsymbol{u}) \\ \text{s.t.} \quad & \mathbb{P}\left[\boldsymbol{G}^u \boldsymbol{u} + \boldsymbol{G}^w \boldsymbol{w} \leq \boldsymbol{g}\right] \geq 1 - \alpha \\ & \boldsymbol{F}\boldsymbol{u} \leq \boldsymbol{f}. \end{aligned} \tag{10.12}$$

10.2.3.2 Scenario-Based Approximation

Unless the uncertainties follow specific distributions, e.g., Gaussian or log-concave, chance constraints problems as (10.12) are generally non-convex and thus numerically difficult to handle [23]. Uncertainties like solar radiation and occupancy do

not usually follow probability distributions that allow us to formulate equivalent deterministic problems and make MPC problems more tractable.

The scenario-based optimization approach [8, 24] provides a way of approximating the solution of chance-constrained optimization problems, and is based on finding the optimal solution under a finite number of sampled outcomes of uncertainty. This approach does not require explicit knowledge of the uncertainty set, as in robust optimization, nor of its probability distribution, as in stochastic programming; the only requirement is that one should be able to extract a sufficient number of independent random samples from the distribution of uncertainty. The number of samples is selected to guarantee the feasibility of the solution so that the solution of the scenario problem has generalization properties, i.e., it satisfies with high probability unseen scenarios. Therefore, the original program is approximated with a deterministic one, called the *scenario problem*, which is obtained from the original by replacing the chance constraint with the S sampled deterministic constraints. By construction, the scenario problem is deterministic and convex and thus it can be solved efficiently by standard numerical algorithms. In our specific HVAC control problem, the scenario approach leads to a simple linear problem to be solved at each time step; we follow this approach and extract a set of S i.i.d. disturbances samples or scenarios, $\boldsymbol{w}_1, \ldots, \boldsymbol{w}_S$, with $\boldsymbol{w}_i := \left[w_i^{\mathrm{T}}(0), \ldots, w_i^{\mathrm{T}}(N-1)\right]^{\mathrm{T}}$, $i = 1, \ldots, S$. These generated scenarios correspond to a set of different realizations of exogenous disturbance variables w which represent weather conditions and occupancy. These quantities are extracted from a learned multidimensional probability distribution trained from historical data by using copulas formalisms, see, e.g., [11–13]. We remark that posing Gaussianity assumptions limit the dependencies that can be captured by restricting the types of admitted behaviors in the tails of marginal distributions. References [11–13] also show that in HVAC control frameworks Gaussianity assumptions may be unrealistic, especially when modeling occupancy or solar radiation effects.

Hence, Problem (10.12) is approximated with the following scenario-based problem:

$$\begin{aligned} \min_{\boldsymbol{u}} \; & J(x(0), \boldsymbol{u}) \\ \text{s.t.} \; & \boldsymbol{G}^u \boldsymbol{u} \leq \boldsymbol{g} - \max_{i=1,\ldots S} \boldsymbol{G}^w \boldsymbol{w}_i \\ & \boldsymbol{F}\boldsymbol{u} \leq \boldsymbol{f}. \end{aligned} \tag{10.13}$$

Recently, authors in [25] have obtained useful results on the closed-loop constraint violations in a scenario-based MPC framework. In this work, these results are used to set a lower bound on the number of scenarios providing guarantees on the probability of constraint violation. Furthermore, since in this manuscript we formulate a cascade of two scenario-based optimization problems, we apply the results provided in [26] to guarantee the feasibility of the cascaded solution of the two individual problems (see Theorem 7 in [26]).

10.2.4 Implicit SMPC Formulation for HVAC Control

We now describe our implicit SMPC formulation by illustrating the control architecture of our SMPC for HVAC systems in Sect. 10.2.4.1 and the two scenario-based optimization problems in Sect. 10.2.4.2 (as for the CO_2-SMPC problem) and in Sect. 10.2.4.3 (as for the T-SMPC problem). We then discuss some experimental results in Sect. 10.2.4.4.

10.2.4.1 Control Architecture

The architecture of the proposed control system is illustrated in Fig. 10.2. Here the indoor temperature and the air CO_2 concentration levels (both to be considered as comfort indicators) are controlled through the ventilation system and radiators, while the latter two elements are actuated using low-level proportional-integral (PI) controllers. The proposed SMPC scheme computes then at each time instant the set points for the low-level controllers using new measurements and updated information about weather and occupancy patterns.

The inputs of our SMPC for HVAC systems are, at every time step: *(i)* occupancy levels, *(ii)* weather conditions, and *(iii)* measurements of the building current state. The output is a heating, cooling and ventilation plan for the next N hours (with N being a prediction horizon chosen by the user when designing the control system). Consistently with the MPC paradigm, at every time step k only the first step of this control plan is applied to the HVAC system. After that, the whole procedure is repeated based on new measurements and updated forecasts and scenarios. This introduces feedback into the system, since the control action is a function of the

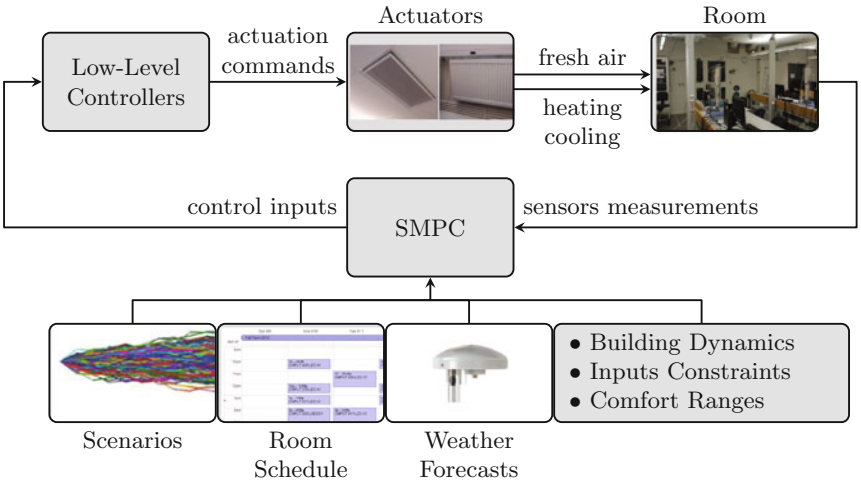

Fig. 10.2 Architecture of the control system implemented on the testbed (reprinted with permission, from [13])

current system state and the currently acting disturbances. In our case the computed outputs are, at every time step k: *(i)* a mass air flow rate $\dot{m}_{\text{venting}}(k)$; *(ii)* a supply air temperature $T_{\text{sa}}(k)$; *(iii)* a radiators mean radiant temperature T_{mr}.

10.2.4.2 CO_2-SMPC Problem

The generic model (10.9) is replaced in this case with (10.5). The CO_2 concentration over the prediction horizon, denoted by $\boldsymbol{y}_{\text{CO}_2}$, can be expressed as a function of the initial state $x_{\text{CO}_2}(0)$ as in (10.10).

The cost function is

$$J_{\text{CO}_2}(u_{\text{CO}_2}(k)) = u_{\text{CO}_2}(k)\Delta k, \tag{10.14}$$

where Δk the sampling period. The bounds on the input $u_{\text{CO}_2}(k)$ are of the form $u_{\text{CO}_2}^{\min} \leq u_{\text{CO}_2}(k) \leq u_{\text{CO}_2}^{\max}$, while the comfort constraints on the indoor CO_2 concentration can be set as $0 \leq y_{\text{CO}_2}(k) \leq y_{\text{CO}_2}^{\max}$. These bounds can be expressed as polytopic constraints $F_{\text{CO}_2} u_{\text{CO}_2}(k) \leq f_{\text{CO}_2}$ and $G_{\text{CO}_2}^{y} y_{\text{CO}_2}(k) \leq g_{\text{CO}_2}^{y}$, respectively.

Constraints (10.4) can be written in a compact form as mixed constraints on inputs and outputs. By expressing $\boldsymbol{y}_{\text{CO}_2}$ as a function of $x_{\text{CO}_2}(0)$, we can write both comfort constraints and mixed constraints on inputs and outputs over the whole prediction horizon as $\boldsymbol{G}_{\text{CO}_2}^{u}\boldsymbol{u}_{\text{CO}_2} + \boldsymbol{G}_{\text{CO}_2}^{w}\boldsymbol{w}_{\text{CO}_2} \leq \boldsymbol{g}_{\text{CO}_2}$, where $\boldsymbol{G}_{\text{CO}_2}^{u}$, $\boldsymbol{G}_{\text{CO}_2}^{w}$ and $\boldsymbol{g}_{\text{CO}_2}$ are matrices of appropriate dimensions.

The CO_2-SMPC problem can thus be formulated as in (10.12):

$$\begin{aligned} \min_{\boldsymbol{u}_{\text{CO}_2}} \; & J_{\text{CO}_2}(x_{\text{CO}_2}(0), \boldsymbol{u}_{\text{CO}_2}) \\ \text{s.t.} \; & \boldsymbol{G}_{\text{CO}_2}^{u}\boldsymbol{u}_{\text{CO}_2} \leq \boldsymbol{g}_{\text{CO}_2} - \max_{i=1,\dots S} \boldsymbol{G}_{\text{CO}_2}^{w}\boldsymbol{w}_{\text{CO}_2,i} \\ & \boldsymbol{F}_{\text{CO}_2}\boldsymbol{u}_{\text{CO}_2} \leq \boldsymbol{f}_{\text{CO}_2}. \end{aligned} \tag{10.15}$$

After solving the CO_2-SMPC problem, we can easily derive $\dot{m}_{\text{venting}}^{\text{CO}_2}(k)$. The current measurement of the indoor CO_2 level is used to compute the control input for the current point in time.

10.2.4.3 T-SMPC Problem

The system model (10.9) is in this case (10.8). The indoor temperature $\boldsymbol{y}_{\text{T}}$ over the prediction horizon can be expressed as a function of the initial state $x_{\text{T}}(0)$ as in (10.10).

The control objective is to minimize the thermal energy use

$$J_{\text{T}}(u_{\text{T}}(k)) = \left(\rho_{\text{venting}} \left| Q_{\text{venting}}(k) \right| + Q_{\text{heating}}(k)\right)\Delta k = \tag{10.16}$$

$$= \left(c^{\text{T}}(k) u_{\text{T}}(k)\right)\Delta k, \tag{10.17}$$

where $u_{\mathrm{T}}(k) := \left[\Delta T_h(k), \Delta T_c(k), \Delta u_h(k), \Delta u_c(k), \Delta T_{h,\mathrm{rad}}(k)\right]$ and $c(k)$ are, respectively, the input and the cost vectors at time k and ρ_{venting} is a factor modeling the higher energy cost of the ventilation system with respect to the radiators in the heating mode.

We define bounds on the input $u_{\mathrm{T}}(k)$ of the form $u_{\mathrm{T}}^{\min} \leq u_{\mathrm{T}}(k) \leq u_{\mathrm{T}}^{\max}$, and on the comfort constraints on the indoor temperature as $0 \leq y_{\mathrm{T}}(k) \leq y_{\mathrm{T}}^{\max}$. Bounds on inputs along with constraints (10.7) can be expressed as polytopic constraints $F_{\mathrm{T}} u_{\mathrm{T}}(k) \leq f_{\mathrm{T}}$, while comfort constraints can be written as $G_{\mathrm{T}}^{y} y_{\mathrm{T}}(k) \leq g_{\mathrm{T}}^{y}$.

Constraints (10.6) can be written in a compact form as mixed constraints on inputs and outputs. By expressing $\boldsymbol{y}_{\mathrm{T}}$ as a function of $x_{\mathrm{T}}(0)$, we can write both comfort constraints and mixed constraints on inputs and outputs over the whole prediction horizon as $\boldsymbol{G}_{\mathrm{T}}^{u}\boldsymbol{u}_{\mathrm{T}} + \boldsymbol{G}_{\mathrm{T}}^{w}\boldsymbol{w}_{\mathrm{T}} \leq \boldsymbol{g}_{\mathrm{T}}$, where $\boldsymbol{G}_{\mathrm{T}}^{u}$, $\boldsymbol{G}_{\mathrm{T}}^{w}$ and $\boldsymbol{g}_{\mathrm{T}}$ are matrices of appropriate dimensions.

The T-SMPC problem can thus be formulated as in (10.12):

$$\begin{aligned} \min_{\boldsymbol{u}_{\mathrm{T}}} \; & J_{\mathrm{T}}(x_{\mathrm{T}}(0), \boldsymbol{u}_{\mathrm{T}}) \\ \text{s.t.} \; & \boldsymbol{G}_{\mathrm{T}}^{u}\boldsymbol{u}_{\mathrm{T}} \leq \boldsymbol{g}_{\mathrm{T}} - \max_{i=1,\ldots,S} \boldsymbol{G}_{\mathrm{T}}^{w}\boldsymbol{w}_{\mathrm{T},i} \\ & \boldsymbol{F}_{\mathrm{T}}\boldsymbol{u}_{\mathrm{T}} \leq \boldsymbol{f}_{\mathrm{T}}. \end{aligned} \tag{10.18}$$

After solving the T-SMPC problem, we can easily derive the control variables $T_{\mathrm{sa}}(k)$, $T_{\mathrm{mr}}(k)$ and $\Delta\dot{m}_{\mathrm{venting}}(k)$. The total air flow rate at the current point in time, k, can be computed as $\dot{m}_{\mathrm{venting}}^{\mathrm{CO_2}}(k) + \Delta\dot{m}_{\mathrm{venting}}(k)$. Current measurements of the temperatures in the room and in the ventilation system are used to compute control inputs for the current point in time.

10.2.4.4 Experimental Evaluation

Here we describe the experimental setup, the KTH HVAC testbed, and discuss experimental results.

Experimental setup

The KTH HVAC testbed is hosted on the KTH main campus and is located in the ground floor of a seven-story office building with a concrete heavyweight structure. The testbed consists of four rooms: a laboratory and three student offices; the results presented in this work refer to the laboratory room, which has a limited windows surface and one external wall, facing southeast. The rooms are all equipped with a Supervisory Control And Data Acquisition (SCADA) and Programmable Logic Controllers (PLCs), a wireless sensor network, an actuator network, and a weather station.

The installed sensors enable continuous monitoring of the status of the system, i.e., CO_2 temperatures, humidity, and external weather conditions as in Fig. 10.3. The implemented platform also gathers data from weather forecasts services and is integrated with the rooms web-based scheduling services of the occupancy (calendars). Occupancy is measured through a photoelectric based people counter.

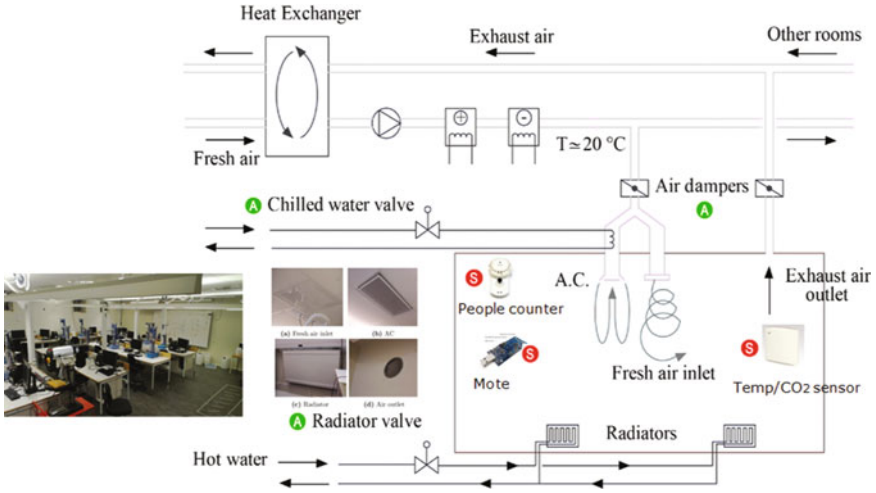

Fig. 10.3 Scheme of the HVAC system of one of the rooms of the KTH HVAC testbed (reprinted, with permission, from [13])

The HVAC system of the rooms consists of a ventilation system supplying fresh air plus a radiator heating system. Air is ventilated into the rooms by a central fan (not controllable in the current experimental setup) running by default between 8:00 and 15:00 during weekdays. A central balanced ventilation system with heat recovery preconditions fresh air from the outdoor environment, distributing it at a temperature of about 20–21°C. Approximately 70% of the total air flow is directly conveyed into the rooms from the central air handling unit, while the remaining part can be further cooled by a local cooling coil. The ventilation airflow is controlled via two dampers that regulate the opening of the inlet and outlet ducts; the ventilation air temperature is controlled actuating on a cooling coil. When the central fan is on, a minimum air flow is distributed into the rooms due to building regulations independently from their occupancy. The heating system uses standard waterborne radiators as heat emission units. Heat is provided by district heating, with supply temperature of the water dependent on the outdoor temperature. Heat emission from radiators is controlled acting on the valve that regulates the hot water flow.

Experimental results

Here we discuss and evaluate the results of experiments performed on the KTH HVAC testbed.

We point out that the thermal model used for control has been implemented in MATLAB and verified against the results provided by IDA-ICE 4.5 [27], a commercial software program for energy and comfort calculations in buildings. Furthermore, the temperature and CO_2 models have been successfully validated against measurements from the testbed [11, 13].

Three different controllers have been tested on the HVAC system in the testbed main room during three different days (see Fig. 10.4):

1. the current practice, which corresponds to a simple control logic with PI control loops and switching logic, indicated in the following by the acronym AHC (the controller from Akademiska Hus, the company managing the building of the testbed);
2. a Deterministic Model Predictive Control (DMPC) neglecting information on the uncertainties in the forecasts, and computing the control inputs by solving the HVAC control problem with deterministic constraints obtained by replacing the unknown disturbances with their forecasts;
3. our SMPC introduced above.

The three controllers have been tested between April and June 2014 for 7 h each day, from 8:00 to 15:00. The sampling time for the MPC-based controllers is 10 min, while the predictions horizon is 8 h. The comfort range of the indoor temperature is [20, 22] °C. The controllers have been tested during spring and summer, when cooling was required.

Figure 10.4 depicts the results of the three controllers tested in 3 days in April and May. The horizontal axis reports the time period of the experiments. Each row

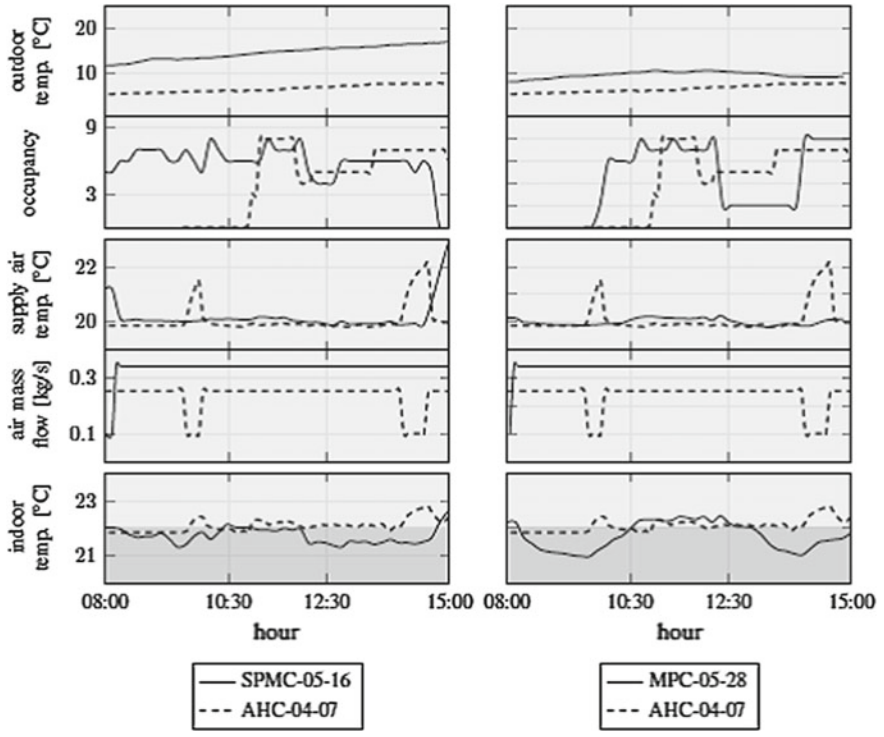

Fig. 10.4 Disturbances, indoor temperature and control input profiles for tests on April 7, May 16 and 28

of the figure depicts the disturbances (i.e., outdoor temperature and occupancy), the control inputs (i.e., supply air temperature and air mass flow) and the controlled indoor temperature. The left column compares results between SMPC and AHC, while the right column shows the results of MPC against AHC. The solid lines of both columns represent disturbances, input and output profiles of MPC-based strategies while the dashed lines are related to the current practice AHC.

The MPC-based controllers clearly improve the thermal comfort with respect to the AHC one: indeed, despite the fact that the MPC-based controllers have to compensate for higher internal gains from occupants and higher outdoor temperatures, they also show almost no violations to the comfort constraints, while AHC yields significant violations of the thermal comfort upper bound. Notice in particular the experiment in the first column of Fig. 10.4, it can be seen that our SMPC had to compensate for a higher outdoor temperature, a more challenging situation when cooling.

The differences in the performance of the two MPC-based controllers thus emphasize the added value of incorporating information on the disturbances that affect the system: the SMPC computes its control inputs based on a worst-case scenario approach, which leads to a more robust behavior against unknown disturbances. As a consequence, the SMPC is able to keep the temperature closer to the upper bound and violates less with respect to the DMPC. The advantages of this behavior are more stressed when occupancy is higher.

In general, we can notice that, when the outdoor temperature and the occupancy are higher, SMPC has better performance in terms of violations of the thermal comfort with respect to the DMPC. See, for instance, the temperature profile resulting from DMPC, represented by the solid line in the right column and the last row of Fig. 10.4: the DMPC is not able to compensate for the occupancy peak at 11:00–12:00 am, resulting in violations of the thermal comfort.

10.2.5 Explicit SMPC Formulation for HVAC Systems

Implicit MPC strategies come with an online computational burden, intensified by the scenario generation procedure. A possible solution is to determine explicitly, off-line, the solution of the MPC optimization problem as a function of the current building state by solving multiparametric programs [9, 10]. In the following, we outline the explicit formulation of the SMPC for HVAC control (10.13).

10.2.5.1 Computing the Explicit Solution

We adopt a two states thermal model of a single thermal zone (or room). We model a thermal zone as a network of two nodes, one accounting for the dynamics of the air within the zone, and the other one accounting for the dynamics of the walls. This model and its validation against measurements are described in detail in [12].

Problems (10.15) and (10.18) can be treated as multiparametric linear problems by considering initial state vectors, respectively, $x_{\mathrm{CO}_2}(0)$ and $x_{\mathrm{T}}(0)$ as vectors of parameters.

By solving the multiparametric CO_2-SMPC and T-SMPC problems, we obtain explicit state-feedback laws that are expressed as PWA functions of the initial state vectors.

Hence, the explicit CO_2-SMPC and T-SMPC control laws have, respectively, the form

$$\begin{array}{rl} u^{E\mathrm{CO}_2}(x) = Q_i^{E\mathrm{CO}_2} x + q_i^{E\mathrm{CO}_2} & \text{if } H_i^{E\mathrm{CO}_2} x_{\mathrm{CO}_2}(0) \leq K_i^{E\mathrm{CO}_2} \\ u^{ET}(x) = Q_j^{ET} x + q_j^{ET} & \text{if } H_j^{ET} x_{\mathrm{T}}(0) \leq K_j^{ET} \end{array}$$

where the polyhedral sets $\mathcal{X}_i^{E\mathrm{CO}_2} := \left\{ H_i^{E\mathrm{CO}_2} x \leq K_i^{E\mathrm{CO}_2} \right\}$ and $\mathcal{X}_j^{ET} := \left\{ H_j^{ET} x \leq K_j^{ET} \right\}$, with $j = 1 \ldots N^{ET}$ are partitions of the set of states, with $i = 1, \ldots, N^{E\mathrm{CO}_2}$ and $j = 1, \ldots, N^{ET}$.

To guarantee that the overall procedure satisfies the requirements on the minimum mass flow needed to maintain comfortable CO_2 levels, we proceed as follows: the set of admissible values of the mass flow is partitioned using standard algorithms (e.g., Lloyd algorithm [28]) and Q quantized values are computed, $\dot{m}^{\mathrm{CO}_2}_{1,\mathrm{quantized}}, \ldots, \dot{m}^{\mathrm{CO}_2}_{Q,\mathrm{quantized}}$. Then, for each $\dot{m}^{\mathrm{CO}_2}_{i,\mathrm{quantized}}$, a corresponding explicit T_i-SMPC problem that takes $\dot{m}^{\mathrm{CO}_2}_{i,\mathrm{quantized}}$ as lower bound on the mass flow is solved.

The scenario-based controller can be then implemented online according to Algorithm 1.

Algorithm 10.1 On-line Implementation

1: **for** $k = 1, 2, \ldots$ **do**
2: measure $x_{\mathrm{CO}_2}(k)$ and $x_{\mathrm{T}}(k)$
3: compute $u^{E\mathrm{CO}_2}\left(x_{\mathrm{CO}_2}(k)\right)$ and derive $\dot{m}^{\mathrm{CO}_2}_{\mathrm{venting}}(k)$
4: identify the quantized value $\dot{m}^{\mathrm{CO}_2}_{i,\mathrm{quantized}}(k)$
5: compute $u^{ET}\left(x_{\mathrm{T}}(k)\right)$ by using the solution of the explicit T_i-SMPC problem and derive the setpoints $\left(\dot{m}_{\mathrm{venting}}(k), T_{\mathrm{sa}}(k), T_{\mathrm{mr}}(k)\right)$
6: send the computed setpoints to the low-level PI controllers
7: **end for**

10.3 Building Generation-Side and Demand-Side Management

As highlighted in Sect. 10.1, smart buildings can integrate not just flexible loads, but also storage systems and generation capabilities. Energy management frameworks for smart buildings should support multiple performance criteria (load shaping, economic costs, comfort, power imbalances minimization), along with more standard

objectives (control of the indoor air quality and thermal comfort), and optimize the flexibility provided by onsite generation (e.g., Photovoltaic (PV)), storage systems, and Demand Response (DR) policies [1] (commonly defined as changes in electricity use by consumers in response to changes in the electricity price over time [29]). Effective energy management with DR policies can help flattening the aggregated demand curve and reducing the number of expensive generation plants used for peak load periods. In recent years, more and more utilities and governments offer programs that provide incentives for residential consumers to adopt on-site distributed generators and energy storage systems [30]. However energy storage devices and renewables are not still common within homes, they are often included in energy management frameworks of future environmentally friendly homes [31].

In this section, we describe a novel MPC-based EMS for smart buildings to optimally manage and coordinate energy supply and demand in multiple houses, taking user preferences into account. The control system computes an optimal energy plan based on forecasts of weather conditions, renewable generation and thermal demand; imbalances can be compensated through the feedback mechanism integrated into our framework. The feedback mechanism introduced through the MPC receding horizon philosophy allows us to compute current power imbalances, and thus take corrective actions to guarantee power balance and user comfort. Smart appliances are included since we consider DR, which can take advantage of the additional flexibility offered by storage devices, to store energy and release it when it is more convenient [32].

We consider a system representing either a residential district made up of several single-family houses with local generation capabilities owning a shared DER, or a smart building composed of apartments with heating systems and storage devices sharing a common Distributed Energy Resource (DER).

We illustrate the modeling and MPC problem formulation for the system described above in Sect. 10.3.1. An extension of this framework, including the user behavior uncertainty in scheduling shiftable appliances, is outlined in Sect. 10.3.2. Lastly, we sketch in Sect. 10.3.3 a distributed approach to solve the problem of coordinating a set of smart appliances located in N apartments sharing an Energy Storage System (ESS).

10.3.1 MPC-Based EMS for Smart Buildings

As mentioned above, we consider a system representing either a residential district or a smart building. The subsystems we account for are then either single-family houses or apartments owning a shared DER and comprising heat pumps, ESSs and both thermal and electrical loads (e.g., heating system, electrical appliances).

We remark that the proposed EMS framework can be easily adapted to other energy systems (e.g., networks of microgrids, industrial facilities) and extended to include other DER and control objectives (e.g., electrical vehicles, fuel cells, emission reduction).

We would like to mention that a virtual experimental testbed has been built for evaluating experimental results, the Virtual MicroGrid Lab [33], where partners from industry and academia have combined resources to develop a virtual laboratory interconnecting partner laboratory premises using secure connections on top of the public Internet. A case study of five residential microgrids is implemented and simulated in the virtual laboratory; simulation results show that the storage devices allow a 10.47% cost savings and the proposed control framework can achieve up to 58.8% cost savings.

In the following, we describe the modeling of the system components and we formulate the MPC problem.

10.3.1.1 Modeling

Here we briefly describe the modeling framework of the considered system.

As depicted in Fig. 10.5, each subsystem is equipped with a Home Energy Management System (HEMS), which is responsible for operating the end-user smart appliances, the local generation devices and the interaction with the grid at the residential level according to the setpoints computed by the control system. The MPC controller is responsible for coordinating the energy sources, and deals with the long-term behavior of the system (e.g., from 10 min to 1 h). This implies that the controller

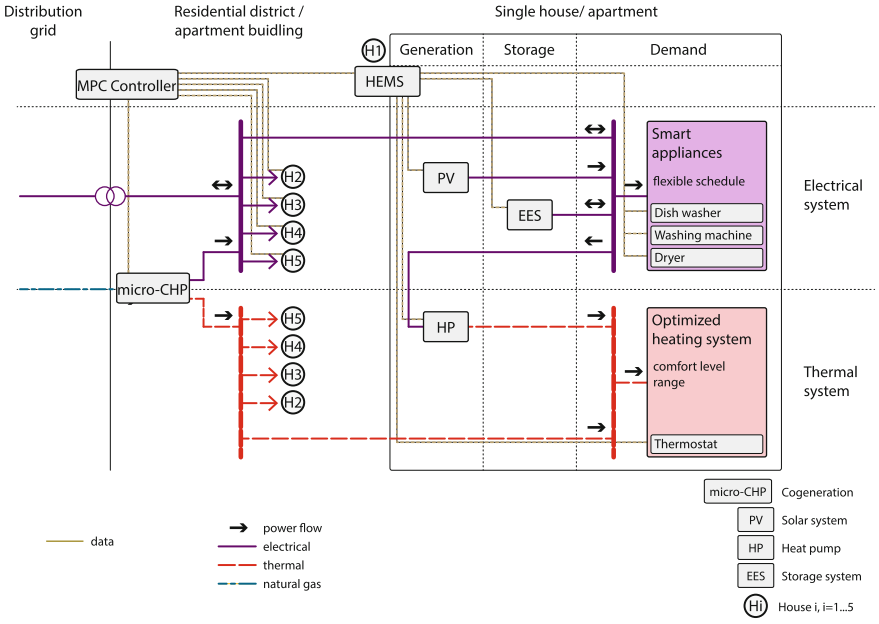

Fig. 10.5 Schematics of the architecture of the system under consideration (reprinted, with permission, from [34])

Table 10.2 Parameters

Parameters	Description
H	Scheduling horizon
$N_{\text{appliance,h}}$	Number of home smart appliances for house h
N_{h}	Number of houses
n_i	Number of energy phases of appliance i
$E_{i,j}$	Energy requirements for energy phase j of appliance i
$\underline{P}_{i,j}$, $\overline{P}_{i,j}$	Bounds on energy phase power
$\underline{T}_{i,j}$, $\overline{T}_{i,j}$	bounds on number of time slots for energy phase j
	of appliance i
$\underline{D}_{i,j}$, $\overline{D}_{i,j}$	Bounds on between-phase delays in the number
	of time slots
TP_i	User time preference interval for appliance i
c_{gas}	Fuel (natural gas) cost for the micro-CHP
$\alpha_{\text{s,h}}$	Storage energy degradation for house h
$c_{\text{s,h}}$	Operating and maintenance cost of the power exchanged with the storage unit for house h
$\eta^{\text{c}}_{\text{s,h}}$, $\eta^{\text{d}}_{\text{s,h}}$	Charging/discharging efficiencies of storage for house h
α_1,α_0,β_1,β_0	Parameters of the micro-CHP model
$P^{\text{peak,h}}$	"Peak signal" for house h (i.e., total slot energy upper bound)
$\underline{P}^{\text{heat}}_{\text{chp}}$, $\overline{P}^{\text{heat}}_{\text{chp}}$	Bounds on micro-CHP thermal power
$\underline{P}^{\text{el}}_{\text{chp}}$, $\overline{P}^{\text{el}}_{\text{chp}}$	Bounds on micro-CHP electrical power
$\underline{P}_{\text{gas}}$, $\overline{P}_{\text{gas}}$	Bounds on micro-CHP gas power
$\underline{P}^{\text{heat}}_{\text{hp,h}}$, $\overline{P}^{\text{heat}}_{\text{hp,h}}$	Bounds on heat pump thermal power to house h
$\underline{P}^{\text{el}}_{\text{hp,h}}$, $\overline{P}^{\text{el}}_{\text{hp,h}}$	Bounds on heat pump electrical power to house h
$\underline{P}_{\text{s,h}}$, $\overline{P}_{\text{s,h}}$	Bounds on the power exchanged with the storage for house h
$\underline{E}_{\text{s,h}}$, $\overline{E}_{\text{s,h}}$	Bounds on the storage energy level for house h

is weakly dependent on the transient behavior of the fast dynamics and a steady-state assumption for the components can be safely made without much loss of accuracy. Thus, the most relevant dynamics are the building thermal dynamics and the storage dynamics.

The forecasts, parameters and decision variables used in the proposed formulation are described, respectively, in Tables 10.2, 10.3, and 10.4 reported in the appendix. For further details on the components modeling we refer the interested reader to the technical report [33].

Forecasts of PV generation are computed by considering efficiency changes due to the given weather data and taking also other losses (e.g., inverter) into account.

We consider two types of loads:

- *thermal loads*, i.e., demand levels related to thermal indoor comfort;
- *electrical loads*, i.e., demand levels related to smart appliances.

Table 10.3 Forecasts

Forecasts	Description
c_{tariff}	Electricity tariff
$\underline{P}_{\text{h}}^{\text{heat}}$, $\overline{P}_{\text{h}}^{\text{heat}}$	Bounds on thermal power demand for house h (corresponding to the thermal comfort range)
$COP_{\text{hp,h}}$	Coefficient of Performance (COP)
$P_{\text{res,h}}$	Power generation from renewables for house h

Table 10.4 Decision and logical variables

Variables	Description
δ_{chp}	Off(0)/on(1) state of the micro-CHP
$\delta_{\text{s,h}}^{\text{c}}$,$\delta_{\text{s,h}}^{\text{d}}$	Storage charging/discharging state for house h
$P_{i,j}$	Power profile for each phase
$x_{i,j}$	Indicator of whether a phase is on or off
$t_{i,j}$	Indicator of whether a transition is happening
$s_{i,j}$	Indicator of whether a phase has been off
$P_{\text{h}}^{\text{grid}}$	Importing(positive)/exporting(negative) power from/to the grid for house h
P_{gas}	Gas power input to the micro-CHP
$P_{\text{chp,h}}^{\text{heat}}$	Micro-CHP thermal power to house h
$P_{\text{chp,h}}^{\text{el}}$	Micro-CHP electrical power to house h
$P_{\text{hp,h}}^{\text{heat}}$	Heat pump thermal power to house h
$P_{\text{hp,h}}^{\text{el}}$	Heat pump electrical power to house h
$P_{\text{h}}^{\text{heat}}$	Thermal power demand for house h
$P_{\text{s,h}}^{\text{c}}$,$P_{\text{s,h}}^{\text{d}}$	Charging/discharging power exchanged with the storage for house h
$E_{\text{s,h}}$	Storage energy level for house h

symbol	*description*
s	scenario index
S	number of scenarios

Thermal Loads

Forecasts of the minimum and the maximum thermal energy required to keep the indoor temperature in the houses within a given comfort range are computed through a dynamic house model based on forecasts of the weather conditions. The house model runs on top of the Apros process simulation software [35]. The model includes the energy dynamics of building structure and indoor temperature and account for the outdoor temperature, the solar radiation and the internal gains from occupants and equipment. A further extension of the described EMS will include the HVAC controller described in the previous section.

Electrical loads

An appliance operation process is made up of sub-processes called energy phases. An energy phase is considered uninterruptible, and it consumes a pre-specified amount of electric energy in order to finish the physical task. Several other technical and user-specified constraints are included in the problem formulation: *(i)* both the power assigned to the energy phase at any time slot and its duration have to take values within a certain range; *(ii)* all energy phases associated with a single appliance must be run sequentially; *(iii)* delays between the energy phases are considered, but the order must be observed; *(iv)* for safety reasons, the total power assigned to all appliances at any moment cannot exceed a limit called peak signal; *(v)* user-specified time preferences are included, requiring that certain appliances should be run within some particular time intervals; *(vi)* user-specified preferences on appliances are modeled, e.g., a certain appliance cannot start before some other appliance finishes. Further details on appliance modeling and technical specifications are provided in [36, 37].

Energy Storage System Modeling

For a storage unit of house h, we consider the following discrete-time model:

$$E_{\mathrm{s,h}}(k+1) = \alpha_{\mathrm{s,h}} E_{\mathrm{s,h}}(k) + \eta^{\mathrm{c}}_{\mathrm{s,h}} P^{\mathrm{c}}_{\mathrm{s,h}}(k) \Delta T - \eta^{\mathrm{d}}_{\mathrm{s,h}} P^{\mathrm{d}}_{\mathrm{s,h}}(k) \Delta T,$$

with $0 < \eta^c, \eta^d < 1$ accounting for the energy losses and $\Delta T = t_{k+1} - t_k$ being a constant sampling time. We introduce binary variables $\delta^{\mathrm{c}}_{\mathrm{s,h}}$,$\delta^{\mathrm{d}}_{\mathrm{s,h}}$ to model the charging and discharging behavior and rule out the possibility of charging and discharging during the same sampling period, as expressed in the following constraints

$$\begin{aligned}
\underline{P}_{\mathrm{s,h}} \delta^{\mathrm{c}}_{\mathrm{s,h}}(k) &< P^{\mathrm{c}}_{\mathrm{s,h}}(k) < \overline{P}_{\mathrm{s,h}} \delta^{\mathrm{c}}_{\mathrm{s,h}}(k) \\
\underline{P}_{\mathrm{s,h}} \delta^{\mathrm{d}}_{\mathrm{s,h}}(k) &< P^{\mathrm{d}}_{\mathrm{s,h}}(k) < \overline{P}_{\mathrm{s,h}} \delta^{\mathrm{d}}_{\mathrm{s,h}}(k) \\
\delta^{\mathrm{c}}_{\mathrm{s,h}}(k) + \delta^{\mathrm{d}}_{\mathrm{s,h}}(k) &\leq 1.
\end{aligned}$$

Bounds on the storage capacity are included in the modeling, along with limits on the total number of daily charging and discharging cycles in order to take the state of health of the ESS into account. Further details on a comprehensive storage modeling are provided in [36, 37].

Heat pump modeling

Heat pumps are devices able to transfer thermal energy by absorbing heat from a cold medium (heat source) and releasing it to a warmer one (heat sink). We consider an electrically operated heat pump, since they are by far the most frequently used. Since thermal efficiency of heat pump systems depends strongly on the temperature difference between heat source and sink as well as the overall operating temperature level, at each time slot, forecasts of the COP based on temperature predictions are integrated in the proposed control framework in order to predict the future heat generation from each heat pump (see [34]).

The following set of constraints model the behavior of the heat pump at each time slot k and for each house h

$$\begin{aligned} P^{\text{heat}}_{\text{hp,h}}(k) &= COP_{\text{hp,h}}(k) \cdot P^{\text{el}}_{\text{hp,h}}(k) \\ \underline{P}^{\text{heat}}_{\text{hp,h}} \leq P^{\text{el}}_{\text{hp,h}}(k) &\leq \overline{P}^{\text{heat}}_{\text{hp,h}} \\ P^{\text{el}}_{\text{hp,h}}(k) &\geq 0, \end{aligned}$$

where $COP_{\text{hp,h}}(k)$ is the forecasted COP of the heat pump at time slots k based on weather forecasts.

Micro-CHP modeling

The component represents a typical micro combined heat and power (micro-CHP) unit. The modeling of the component adopts a data-driven approach, where data from a real-world deployment was used [38], in combination with machine-learning and Big Data techniques (see [34]). The micro-CHP model is:

$$\begin{aligned} P^{\text{el}}_{\text{chp}} &= \alpha_1 \cdot P_{\text{gas}} + \alpha_0 \\ P^{\text{heat}}_{\text{chp}} &= \beta_1 \cdot P_{\text{gas}} + \beta_0. \end{aligned} \tag{10.19}$$

10.3.1.2 MPC Problem Formulation

This section outlines the MPC problem formulation. The optimization problem consists of taking decisions on how to optimally schedule production by generators, storage, as well as controllable loads, to cover the system demand and minimize the generation costs and the cost of imported electricity from the distribution grid in the next hours or day. Supply and demand of electrical and thermal energy are both modeled and handled. The thermal energy is required to provide the needed thermal comfort to the house occupants, while the electrical energy is needed to run the smart appliances and the heat pump. The natural gas is required to run the shared micro-CHP.

At each MPC iteration, the problem is solved based on weather forecasts and the current system conditions. The computed optimal decision is then adjusted according to the actual values of the photovoltaic generation and of the heating requirements from the subsystems. Hence, corrective actions and the corresponding costs are taken in order to cope with potential imbalances. At the next time step, the MPC problem is solved again based on updated forecasts and system condition.

The MPC problem can be formulated as a Mixed Integer Linear Program (MILP) optimization problem. We point out that all the models and constraints described in Sect. 10.3.1.1 are constraints of the MPC problem. We next define the cost function and additional constraints included in the optimization problem to be solved at each MPC iteration. Further details can be found in [34].

Cost function

The aim is to minimize the cost of satisfying both the thermal and electrical loads, hence the objective function is

$$\min \sum_{k=1}^{H} \Big[\sum_{h=1}^{N_\mathrm{h}} \left(c_\mathrm{tariff}(k) \cdot P_\mathrm{h}^\mathrm{grid}(k) + c_\mathrm{s,h} \cdot (P_\mathrm{s,h}^\mathrm{c} + P_\mathrm{s,h}^\mathrm{d}) \right) + c_\mathrm{gas} \cdot P_\mathrm{gas}(k) \Big] \Delta T.$$

Electrical and thermal power balance

The electrical and thermal power balances at each house need to be satisfied. At the current point in time, k, if an appliance is running, the power assigned to the current energy phase by the optimization problem solved at the previous time slot must be considered as a critical load for the current time slot, which cannot be rescheduled and has to be satisfied, since an energy phase is uninterruptible. We denote this amount of power for the house h as $P_\mathrm{assigned,h}(k)$.

The balance between electrical energy production and consumption to be met at each time k for house h, $\forall h, k$ is

$$\sum_{i=1}^{N_\mathrm{appliance,h}} \sum_{j=1}^{n_i} P_{i,j}(k) + P_\mathrm{assigned,h}(k) + P_\mathrm{s,h}^\mathrm{c} - P_\mathrm{s,h}^\mathrm{d} + P_\mathrm{hp,h}^\mathrm{el} + P_\mathrm{chp,h}^\mathrm{el} - P_\mathrm{res,h} = P_\mathrm{h}^\mathrm{grid}.$$

Regarding the thermal energy balance, three energy sources have to be taken into account to fulfill the thermal requirements: the heat pump, the micro-CHP and the waste heat generated by running appliances. Studies suggest that 70% of regular household electric use contributes to the household's heat demand [39].

The balance between thermal energy production and use to be met at each time k for house h, $\forall h, k$ is

$$\underline{P}_\mathrm{h}^\mathrm{heat} \leq 0.7 P_\mathrm{assigned,h}(k) + P_\mathrm{hp,h}^\mathrm{heat} + P_\mathrm{chp,h}^\mathrm{heat} \leq \overline{P}_\mathrm{h}^\mathrm{heat}. \tag{10.20}$$

We remark that the thermal energy demand is optimized through (10.20) such that the indoor temperature in each house is within a given comfort range.

Micro-CHP model

The micro-CHP is driven by natural gas and generates both electric and thermal power. The following set of constraints model the behavior of the shared micro-CHP at each time slot k:

$$\begin{aligned}
\underline{P}_\mathrm{chp}^\mathrm{el} \cdot \delta_\mathrm{chp}(k) \leq P_\mathrm{chp}^\mathrm{el}(k) \leq \overline{P}_\mathrm{chp}^\mathrm{el} \cdot \delta_\mathrm{chp}(k) \\
\underline{P}_\mathrm{chp}^\mathrm{heat} \cdot \delta_\mathrm{chp}(k) \leq P_\mathrm{chp}^\mathrm{heat}(k) \leq \overline{P}_\mathrm{chp}^\mathrm{heat} \cdot \delta_\mathrm{chp}(k) \\
\underline{P}_\mathrm{gas} \cdot \delta_\mathrm{chp}(k) \leq P_\mathrm{gas}(k) \leq \overline{P}_\mathrm{gas} \cdot \delta_\mathrm{chp}(k)
\end{aligned}$$

$$\sum_{h=1}^{N_h} P_{\text{chp,h}}^{\text{el}}(k) = P_{\text{chp}}^{\text{el}}(k)$$
$$\sum_{h=1}^{N_h} P_{\text{chp,h}}^{\text{heat}}(k) = P_{\text{chp}}^{\text{heat}}(k)$$
$$P_{\text{chp,h}}^{\text{heat}}(k) \geq 0$$
$$P_{\text{chp,h}}^{\text{heat}}(k) \geq 0,$$

where $P_{\text{chp}}^{\text{el}}$ and $P_{\text{chp}}^{\text{heat}}$ are defined according (10.19). The constraints above guarantee that the thermal and the electrical power outputs of the micro-CHP are properly shared among the houses and the bounds on the power generation and on the gas power are not exceeded.

Interaction with the grid

The following constraint governs the interaction with the distribution grid

$$-P^{\text{peak,h}} <= P_{\text{h}}^{\text{grid}} <= P^{\text{peak,h}}.$$

The peak signal is provided by the external power grid operator, which can be a demand response signal. The houses have the possibility to sell power to the grid (i.e., $P_{\text{h}}^{\text{grid}}$ can be negative).

10.3.2 Modeling User Behavior Uncertainty

The MPC problem described in Sect. 10.3.1 can be extended by taking into account the user behavior uncertainty in scheduling shiftable appliances. The idea is to map the uncertainty on the decision variables (e.g., starting time of appliances) to an equivalent uncertainty in the weighted sum tariff, which is illustrated in Fig. 10.6. Deviating from starting times x_1 and x_2 by at most M time slots ($M\,\Delta t$) turns into a variability of the tariff by at most Δy_1 and Δy_2, respectively. The parameter M can then be defined based on empirical models of the users, e.g., trained from historical data.

Deviating from the optimal start time of appliances can be considered as variability in the tariff curve. A reasonable expression for defining this uncertainty for each time slot k,i.e., ε^k, is

$$\varepsilon^k = \frac{\max(C_\lambda^k, \sum_{i=k-M}^{k+M} \frac{C_\lambda^i}{2M+1}) - C_\lambda^k}{\max(C_\lambda^k, \sum_{i=k-M}^{k+M} \frac{C_\lambda^i}{2M+1})}$$

which is a function of the tariff curve within an interval of $\pm M\,\Delta t$ minutes in the neighborhood of time slot k.

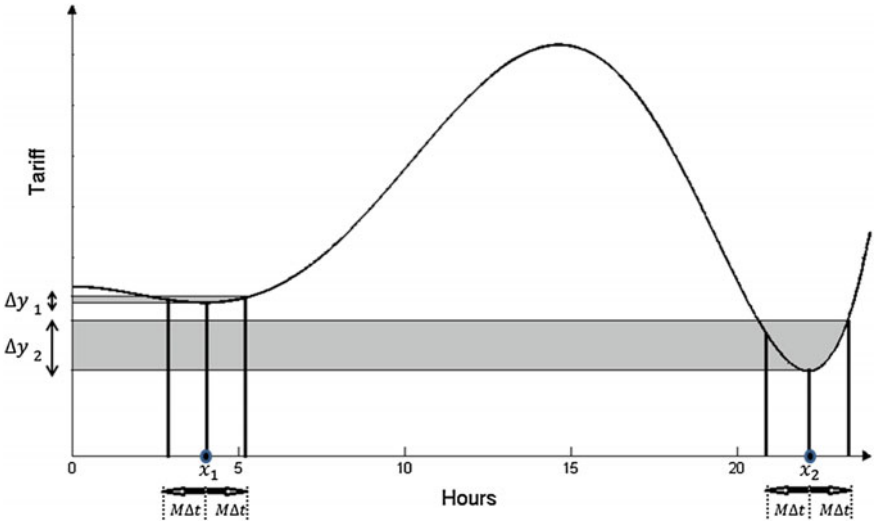

Fig. 10.6 Converting the user behavior uncertainty to tariff uncertainty (reprinted, with permission, from [36])

When considering uncertain parameters in the cost function, a robust approach can be applied in order to obtain schedules of shiftable loads that are less sensitive to uncertainty in the user preferences. A robust solution should be feasible in all scenarios that uncertain parameters variations could define, i.e., all the possible tariff curves described by ε^k. This comes at the cost of a degradation of the objective value, which could be excessive as some of the uncertain scenarios rarely occur. This increase in cost over the nominal solution is the so-called *price of robustness* [40]. In order to prevent overly conservative solutions, the robust optimization approach described in [41, 42] is applied, which considers a tunable degree of robustness. In this formulation, the degree of uncertainty and the level of conservatism of the solution, and the increase in cost, can be regulated by a parameter. The authors in [40, 41] prove that the obtained robust solution will be feasible with high probability. Details on this robust scheduling framework for shiftable loads can be found in [36].

We remark that the proposed framework can be generally applied to other scenarios where different sources of uncertainty and different optimization criteria must be considered. For instance, ε^k can represent the variation from the day-ahead price at time slot k in the real-time energy market, while different optimization criteria can account for the user comfort or the demand peak reduction.

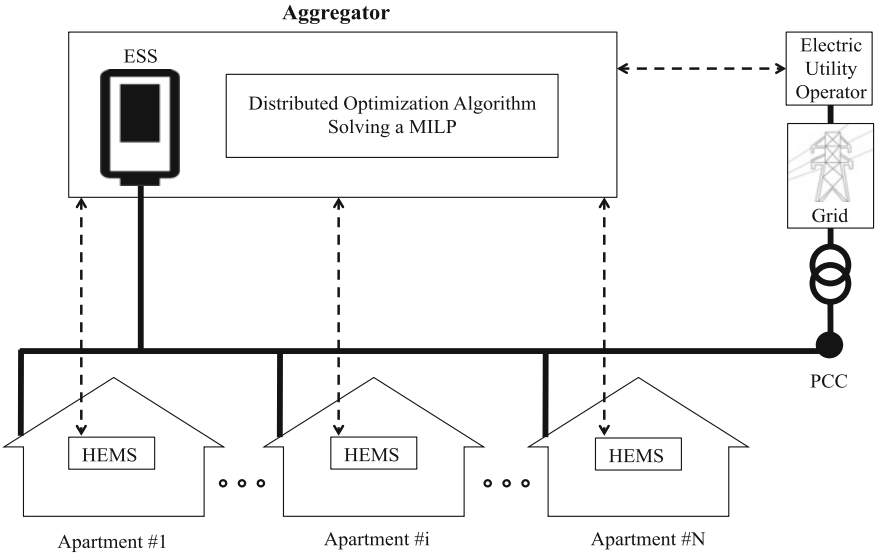

Fig. 10.7 Schematic of interconnected apartments and aggregator (reprinted, with permission, from [37])

10.3.3 A Distributed Approach for Coordinating Shiftable Loads and Storage Systems

When the number of subsystems increases, the centralized approach described so far can be prohibitive and a reasonable solution is to design distributed control architectures, which allow more flexibility in operation and simplified design and tuning.

In this section, we outline a distributed approach to solve the problem of coordinating a set of smart appliances located in N apartments sharing an ESS, as shown in Fig. 10.7. Each apartment can profit from the use of the shared storage while technical and operational constraints, as well as user preferences, are satisfied. Since storage devices are still expensive, a reasonable solution to afford the expense and benefit from the use of an ESS would be to share it among several consumers. Therefore, households should be coordinated by an aggregator, which acts as mediators between users and the utility operator [43]. In order to manage a large set of appliances, we propose an iterative hierarchical approach. We distribute the decision-making mechanism by formulating problems at apartment and aggregator levels. Each apartment is equipped with an HEMS for scheduling the shiftable loads by taking the user preferences and all the technical and operational constraints into account. The local HEMSs are coordinated by the aggregator in order to provide economical incentives to the users on reshaping their demand profiles, guaranteeing that the benefits of using a shared resources are fairly allocated to the users. The framework includes the possibility of buying/selling from/to the distribution grid. The steps of the pro-

posed algorithm are detailed in Algorithm 2. In the initialization step, the aggregated demand profile is computed by the aggregator considering the overall energy requirements from the users, the shared ESS technical and operational constraints, and the interaction with the grid, while each user sends to the aggregator the preferred individual energy profile based on their own needs and preferences, without accounting for the shared resources. The maximum profit obtainable by optimally utilizing the shared resource is then calculated. At subsequent iterations, the aggregator requires each user to shift their energy demand taking also their preferred profile into account, while each individual user aims at optimizing their shiftable load schedule accounting for the requests from the aggregator, based on pre-arranged incentives and penalties. The profit obtainable by the use of the shared resource and the interaction with the grid is calculated at each iteration and equally allocated to the users. Problems at user levels aim at minimizing the energy costs, while the problem at aggregator level maximizes the overall profits. The algorithm terminates when either all the users accept the energy shift requests, or when a maximum number of iterations is reached. The solution computed at each iteration $l \geq 2$ is then guaranteed to be feasible and to ensure fair allocation of profits.

Algorithm 10.2 Distributed algorithm

1: Initialization and computation of the aggregated demand profile
2: **for** $l = 1, 2, \ldots,$ MaxIteration **do**
3: each user level HEMS computes and sends its preferred power profile to the aggregator
4: the aggregator calculates the optimal power shift requests aiming at maximizing the overall profits
5: the aggregator calculates the individual user profits
6: based on these individual profits, each user adjusts its own power profile
7: if all the users accept the power shifts requested by the aggregator then stop, otherwise compute a new aggregated power profile and repeat the cycle
8: **end for**

Preliminary simulation results considering four apartments with three appliances and one shared storage device show that the electricity cost resulting from the final iteration of Algorithm 2 is only 1.3% higher than the centralized optimal solution. On the other hand, the computational time has decreased by two orders of magnitude with respect to the solution time of the centralized formulation.

We point out that the proposed algorithm is suitable for model predictive control frameworks and it can be adapted to provide DR services to the grid operator. Further details can be found in [37].

10.4 Smart Building Demonstrators

In this section, we briefly describe three demonstrators located in Sweden and UK that support ongoing research activities and experiments on EMS for smart buildings:

1. the *Live-In Lab*, a platform for research, development and education in the building sector;
2. the *Manchester Corridor*, the Manchester's cosmopolitan hub and world-class innovation district;
3. the *SICS ICE*, a large-scale testing and experimentation data center facility that supports fully flexible experiments.

10.4.1 KTH Live-In Lab

The KTH Live-In Lab is a platform for research, testing and education to promote innovation in the building sector and it consists of both virtual and physical test environments.

The Live-In Lab consists of a set of three residential buildings, currently under construction, for approximately 300 studio apartments; it is located in the main campus at KTH, Stockholm, Sweden. Heating and cooling power to the buildings are provided by ground-source heat pumps. Heat is distributed airborne to the apartments through a TermoDeck^{TM} [44] system that provides ventilation and heat distribution at the same time. In the TermoDeck^{TM} system, air for ventilation is delivered through pipes embedded in the concrete slabs, allowing pre-heating or pre-cooling of the slabs before air is introduced in the living spaces; these features make it crucial for efficient energy management to effectively control the delays introduced by the thermal masses. Electricity is generated locally with PV panels installed on the flat roof, and the installation of storage systems, in particular batteries for electricity, is under discussion.

The buildings comprise so-called Passive and Active parts. The Passive part accounts for the majority of the floor area and is designed to be extensively equipped with state-of-the-art sensor devices to accurately log indoor and outdoor environmental parameters (e.g., temperature, humidity, light, etc.) for continuous and real-time monitoring of indoor comfort and energy use. In the initial phase of the project, the Passive part will be used only for monitoring. The Active part accounts for approximately 300 m^2 and will be used for more active testing: the experimental setup, including the layout of the apartments comprised in this area, will be periodically changed, allowing a holistic approach to research in buildings. The Active part has a dedicated heating and cooling system and the energy is provided with a separate heat pump and boreholes; advanced monitoring and control will be tested and fine-tuned there to be then applied to the rest of the building.

10.4.2 Manchester Corridor

The Corridor is Manchester's innovation district, a unique business location at the heart of the knowledge economy, generating around 20% of the city's economic

output. It covers some 243 hectares, with a 60000-strong workforce (over 50% are employed in knowledge-based sectors), 72000 students and is the location of the largest clinical academic campus in Europe. It is home to a dense clustering of innovative science and technology businesses, world-class research centers, universities, leading NHS trusts, with a large-scale and transformational infrastructure investment committed to 2020. It provides an ideal testbed for innovation as a microcosm of city activity, driven by the thought leaders on its doorstep and in its institutions.

Corridor Manchester is working toward becoming one of the most sustainable urban locations in Europe and an exemplar for other cities. One of the main objective is to reduce the carbon footprint through the more sustainable management of energy and waste. The Corridor Manchester area is currently one of the demonstrator sites for the Triangulum project [45], a Horizon 2020 Lighthouse project running until 2019, to demonstrate smart green growth across energy, mobility, and ICT. The Innovate UK Internet of Things City Demonstrator project, CityVerve [46], will also be taking place in the Corridor Manchester area with Environment & Energy being a key theme within this project.

10.4.3 SICS ICE

The Swedish Institute for Computer Science (SICS) Infrastructure and Cloud data center test Environment (ICE) research data center project [47] aims at supporting universities and industries with a large-scale data center infrastructure and cloud facility to be used for research, testing and demonstration purposes, especially on topics related to energy efficient software, hardware and infrastructure management (thus also its HVAC systems). The data center can be used by anybody with the formula pay-per-usage to perform tests and experimentation, and enables us to perform large-scale tests to generate realistic data.

The ICE data center is composed of different modules located in neighboring rooms and dedicated to different types of potential tests. Upon completion, forecasted in 2017, ICE will host around 5000 servers plus all the infrastructure needed to support running these devices (e.g., batteries for Uninterruptible Power Supply (UPS) purposes, Computer Room Air Conditioning (CRAC) units, Supervisory Control And Data Acquisition (SCADA) systems, and data visualization facilities) for a total of approximately 2MW peak electrical power consumption.

The facility is located in the municipality of Luleå, in northern Sweden, a favorable location for placing data centers due to the extensive optic fiber capacity, the positive local electrical energy balance (mainly based on renewable energies), and the extreme stability and redundancy of the local electrical network.

As specified in Sect. 10.5, this facility can be used for performing tests related to the coordination of the electrical loads of different buildings. The facility supports remote experimentation, in the sense that researchers can deploy control software and perform experiments remotely.

10.5 Coordinating Data Centers and Buildings for a More Effective Load Management

Data centers are "facilities that centralize an organization's Information Technology (IT) operations and equipment, and where they store, manage, and disseminate their data" [48]. In practice, they are facilities hosting massive amount of computer systems running IT applications, and they can be placed in containers, in dedicated rooms, or even in dedicated buildings.

We can schematize a data center as in Fig. 10.8. IT requests are processed by the various servers, and this produces heat that must be rejected to prevent overheating and thus failure of the servers. An essential component in the control of a data center is played by the IT scheduling algorithm, that decides which server should process a certain IT load. The importance of the IT scheduler can be appreciated noticing the usual structure of an air-cooled data center[1] in Fig. 10.9a and b: allocating IT loads in a place that is currently overheated or difficult to cool may induce hot-spots (and thus failures) and thermal inefficiencies. The IT allocation should thus account also for the thermal dynamics in a data center.

Single data centers may reach electrical power consumptions of more than 100 MW [49] and have industrial-scale operations. They thus have big impacts world-wide: for example, in Europe in 2013 data centers accounted for 3% of the total electric energy consumption (for corresponding emissions of 38.6 million metric tons of CO_2) [50], and it is moreover forecast that by 2020 in Europe 60 other large data centers with more than 1000 servers racks will be built.

Depending on the data center structure and technology, cooling of the server halls accounts for up to 40% of the electrical consumptions. Heat recovery is not yet a widespread solution in data centers management, since the currently dominant cooling strategy is indeed air-based with exhaust coolants having a quite low exergy (air up to 45 °C and with a dew point between 5.5 and 15 °C). A noticeable exception to this trend is the *open district heating* project in Stockholm [51], where data centers from different companies (e.g., Ericsson) are currently providing heat to the district heating system; the exergy of the exhausts is in this case topped up by means of heat pumps. Forecasts are that in the next decade more and more data centers will switch to liquid cooling technology (due to higher energy density servers, that will eventually demand liquid cooling) and thus be integrated into the district heating networks.

10.5.1 Data Centers as Smart Buildings

Data centers can play several different schemes typical of residential smart buildings. Indeed:

[1] Same considerations can be drawn in liquid-cooled data centers.

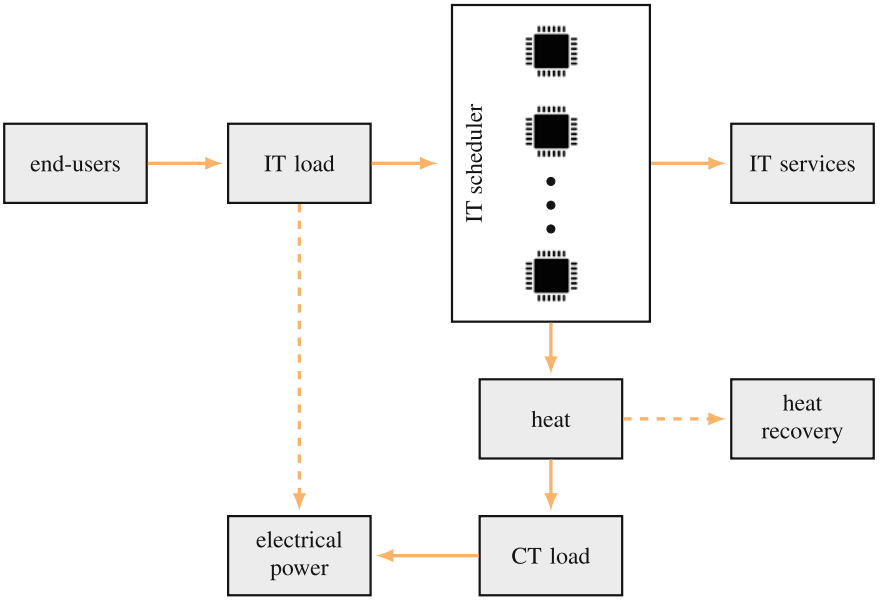

Fig. 10.8 Schematic representation of the operations involved in a data center. Users require some IT services, that are executed by the servers. The corresponding IT load is sorted by the IT scheduler that associates a certain load to a certain physical server. The server thus generates heat that may be recovered or rejected by the Cooling Technologies devices. Both servers and CT devices use electrical power

when considered as elements of the electrical grid, data centers can provide ancillary services like load shifting and load shedding. Indeed data centers' electrical consumptions are mainly due to running the servers and the infrastructure for cooling the servers. Given that it is possible to play pre-cooling schemes like in other smart residential buildings, it is thus possible to perform load shifting and load shedding in data centers in a similar way one does it in other smart buildings;

when considered as elements of the thermal grid, data centers can sometimes act as deferrable prosumers: data centers may figure in this case either in the production or in the consumption sides of the network, especially when connected to cooling grids. In any case pre- and post- cooling, plus temporal shift of deferrable IT loads means to defer thermal production/consumption loads;

when considered as elements of the information grid: moving photons is cheaper than moving electrons. Under favorable electricity price conditions, networks of data centers may use the Internet to communicate and potentially exchange tasks among them, an operation commonly referred to as *geographical load balancing*. Geographical load balancing thus does not just shift IT loads from one location to an other, but also electrical load requests and potential thermal generation capability.

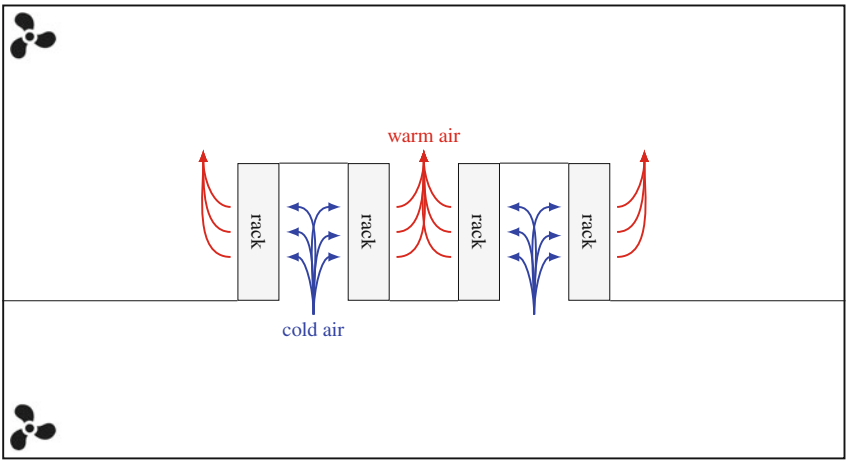

(a) Schematic representation of the typical organization of an air-cooled computer room: warm and cold aisles alternate each other so to diminish disturbances in the cold-air generation unit.

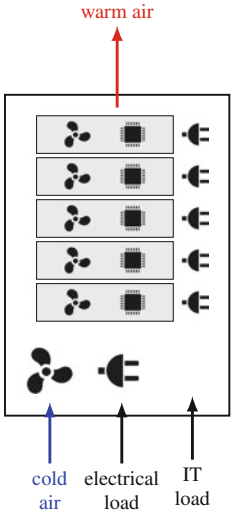

(b) Schematic representation of the typical organization of an air-cooled computer rack: servers are piled on each other so to diminish disturbances in the cold-air generation unit.

Fig. 10.9 **a** Schematic representation of the typical organization of an air-cooled computer room: warm and cold aisles alternate each other so to diminish disturbances in the cold-air generation unit **b** Schematic representation of the typical organization of an air-cooled computer rack: servers are piled on each other so to diminish disturbances in the cold-air generation unit

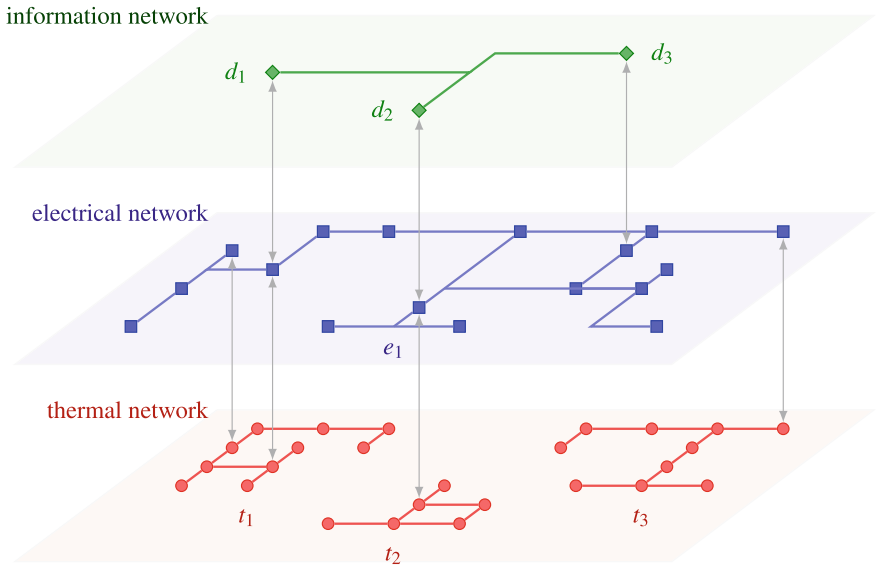

Fig. 10.10 Data centers are consumers in the electrical network, are potential producers in the thermal network, and are prosumers in the information network

The schemes listed above explain why data centers can act as bridges between three types of networks: electrical, thermal and information networks, as graphically shown in Fig. 10.10. This means that data centers are viable players in the smart city environment: obviously, depending on the data center type and electrical/thermal network conditions, one may interplay different types of coordination and synergies. The simplest one is when a single building contains a data center room, as in [52], where heat recovery and electric consumptions can be coordinated directly at a single building's level. More complicated situations may instead require networked control strategies.

10.6 Conclusions and Future Directions

Implementing the next-generation smart energy grids requires buildings that can manage flexible loads, multiple performance criteria, local generation, storage systems and DR policies. These buildings, moreover, shall embed user comfort and preferences during their daily operations. All these requirements entail the need of control schemes that are predictive and allow seamless coordination among different entities. Buildings can indeed help flatten the aggregated demand curve in the electrical network and thus reduce the number of expensive generation plants used for peak load periods.

A natural scheme for optimally operating buildings while accounting for all these aforementioned requirements is MPC, since it allows for flexibility in the design of control objectives.

In this chapter we showed how the basic idea of using a MPC strategy for the management of a smart building can be further refined following some specific directions: the first is taking into account uncertainties, i.e., making the control scheme robust against imprecise models or imprecise knowledge about the future. Numerical experiments performed in daily-life conditions then showed that our approach of following a scenario-based SMPC approach led to effective results in terms of energy savings versus keeping comfortable conditions in the building.

The second direction is formulating the controller so that its implementation complexity is sufficiently low to be implementable in real-world situations. Also in this case, we performed numerical experiments and found that converting the implicit MPCs mentioned above into their explicit versions was leading to effective control schemes.

Furthermore, we described how local generation and storage systems can be integrated into a building energy management framework.

Ongoing and future studies aim at extending the proposed EMS framework to other energy systems and additional DER and control objectives. In particular, it is possible to design distributed, integrated and holistic approaches for the management of networks of thermal and electrical energy systems in coordination with network operators. With this approach the overall energy management problem can be solved in a distributed fashion, aiming to compute feasible solutions to the energy management problem addressing the issue of scalability and taking advantage of opportunities afforded by flexibility services and distributed generation.

References

1. Annaswamy AM, Amin M (2013) IEEE vision for smart grid controls: 2030 and beyond. In: IEEE vision for smart grid controls: 2030 and beyond, pp 1–168, June 2013
2. European Commission (2008) Debate Europe-building on the experience of plan D for democracy, dialogue and debate, European Economic and Social Committee and the Committee of the Regions, COM 158/4, Brussels
3. Costa A, Keane MM, Torrens JI, Corry E (2013) Building operation and energy performance: monitoring, analysis and optimisation toolkit. Appl Energy 101:310–316
4. Chua K, Chou S, Yang W, Yan J (2013) Achieving better energy-efficient air conditioning - a review of technologies and strategies. Appl Energy 104:87–104
5. Morari M, Lee J, Garcia C (2001) Model predictive control. Prentice Hall
6. Treado S, Chen Y (2013) Saving building energy through advanced control strategies. Energies 6(9):4769–4785
7. Sturzenegger D, Gyalistras D, Gwerder M, Sagerschnig C, Morari M, Smith RS (2013) Model predictive control of a Swiss office building. In: Clima-RHEVA world congress, pp 3227–3236
8. Calafiore G, Campi M (2008) The scenario approach to robust control design. IEEE Trans Autom Control 51(5):742–753
9. Alessio A, Bemporad A (2009) A survey on explicit model predictive control. Springer, Berlin. ISBN 9783642010934

10. Bemporad A, Borrelli F, Morari M (2002) Model predictive control based on linear programming~ the explicit solution, Automatic Control Laboratory, ETH, Zurich, Switzerland, Technical report
11. Parisio A, Varagnolo D, Risberg D, Pattarello G, Molinari M, Johansson KH (2013) Randomized model predictive control for HVAC systems. In: Proceedings of the 5th ACM Workshop on Embedded Systems For Energy-Efficient Buildings, ser. BuildSys'13. ACM, New York, NY, USA, pp 19:1–19:8. ISBN 978-1-4503-2431-1
12. Parisio A, Fabietti L, Molinari M, Varagnolo D, Johansson KH (2014) Control of HVAC systems via scenario-based explicit mpc. In: 53rd IEEE conference on decision and control, pp 5201–5207, December 2014. ISSN 0191-2216
13. Parisio A, Varagnolo D, Molinari M, Pattarello G, Fabietti L, Johansson KH (2014) Implementation of a scenario-based MPC for HVAC systems: an experimental case study. IFAC Proc 47(3):599–605
14. Gwerder M, Toedtli J (2005) Predictive control for integrated room automation. In: Clima - RHEVA world congress
15. Gwerder M, Boetschi S, Gyalistras D, Sagerschnig C, Sturzenegger D, Smith R, Illi B (2013) Integrated predictive rule-based control of a swiss office building. In: 11th REHVA world congress clima
16. Haniff MF, Selamat H, Yusof R, Buyamin S, Ismail FS (2013) Review of HVAC scheduling techniques for buildings towards energy-efficient and cost-effective operations. Renew Sustain Energy Rev 27:94–103
17. Širokỳ J, Oldewurtel F, Cigler J, Prívara S (2011) Experimental analysis of model predictive control for an energy efficient building heating system. Appl Energy 88(9):3079–3087
18. Ma Y, Matusko J, Borrelli F (2015) Stochastic model predictive control for building hvac systems: complexity and conservatism. IEEE Trans Control Syst Technol 23(1):101–116
19. Maasoumy M, Razmara M, Shahbakhti M, Vincentelli AS (2014) Handling model uncertainty in model predictive control for energy efficient buildings. Energy Build 77:377–392
20. Dong B, Lam KP, Neuman C (2011) Integrated building control based on occupant behavior pattern detection and local weather forecasting. In: Building simulation, pp 193–200
21. O'Neill Z, Narayanan S, Brahme R (2010) Model-based thermal load estimation in buildings. In: SimBuild, pp 474–481
22. Aglan HA (2003) Predictive model for CO_2 generation and decay in building envelopes. J Appl Phys 93(2):1287–1290
23. Kall P, Mayer J (2005) Stochastic linear programming: models, theory, and computation. Springer
24. Calafiore G (2010) Random convex programs. SIAM J Opt 20(6):3427–3464
25. Schildbach G, Fagiano L, Frei C, Morari M (2014) The scenario approach for stochastic model predictive control with bounds on closed-loop constraint violations. CoRR abs/1307.5640v2
26. Margellos K, Prandini M, Lygeros J (2014) On the connection between compression learning and scenario based optimization. CoRR abs/1403.0950
27. Equa Simulation AB, IDA-ICE. http://www.equa.se/en/, August 2016
28. Sabin MJ, Gray R (1986) Global convergence and empirical consistency of the generalized Lloyd algorithm. IEEE Trans Inf Theor 32(2):148–155
29. Singh S, Ostergaard J (2010) Use of demand response in electricity markets: An overview and key issues. In: 2010 7th international conference on the European energy market (EEM), pp 1–6
30. Bird L, Reger A, Heeter J (2012) Distributed solar incentive programs: recent experience and best practices for design and implementations, NREL/TP-6A20-56308, National Renewable Energy Laboratory, Technical report
31. Beaudin M, Zareipour H (2015) Home energy management systems: a review of modelling and complexity. Renew Sustain Energy Rev 45:318–335
32. Khan AA, Razzaq S, Khan A, Khursheed F, Owais (2015) HEMSs and enabled demand response in electricity market: an overview. Renew Sustain Energy Rev 42:773–785

33. EIT - ICT Labs, Virtual micro grid laboratory. http://www.eitictlabs.eu/evsgl/areas-of-application/supporting-sub-projects/virtual-micro-grid-lab/
34. Parisio A, Wiezorek C, Kyntäjä T, Elo J, Johansson KH (2015) An mpc-based energy management system for multiple residential microgrids. In: 2015 IEEE international conference on automation science and engineering (CASE), pp 7–14, August 2015
35. Apros. http://www.apros.fi/en/
36. Paridari K, Parisio A, Sandberg H, Johansson KH (2016) Robust scheduling of smart appliances in active apartments with user behavior uncertainty. IEEE Trans Autom Sci Eng 13(1):247–259
37. Paridari K, Parisio A, Sandberg H, Johansson KH (2015) Demand response for aggregated residential consumers with energy storage sharing. In: 2015 54th IEEE conference on decision and control (CDC), pp 2024–2030, December 2015
38. Sviluppo T. http://www.trentinosviluppo.com/Contenuti-istituzionali/News/News/2012/Crisalide-a-Roncegno-nasce-l-isola-cogenerativa
39. Levin P (2009) Brukarindata för energiberäkningar i bostäder. Technical, report, SVEBY
40. Bertsimas D, Sim M (2004) The price of robustness. Oper Res 52:35–53
41. Bertsimas D, Sim M (2003) Robust discrete optimization and network flows. Math Program 98:49–71
42. Floudas C (1995) Nonlinear and mixed-integer programming-fundamentals and applications. Oxford University Press, Oxford
43. Gkatzikis L, Koutsopoulos I, Salonidis T (2013) The role of aggregators in smart grid demand response markets. IEEE J Sel Areas Commun 31:1247–1257
44. Termodeck, TermoDeck^{TM}. http://www.termodeck.com/, August 2016
45. Triangulum project. http://triangulum-project.eu/, Triangulum
46. Cityverve project. http://www.cityverve.org.uk/, CityVerve
47. S.I. for Computer Science (2015) SICS infrastructure and cloud data center test environment. TODO
48. Google (2016) Definition of a data center, retrieved from the web. TODO
49. Facebook. www.datacenterknowledge.com/inside-facebooks-lulea-data-center/
50. The Boston Consulting Group (2014) Digital Infrastructure and Economic Development: An impact assessment of Facebook's data center in Northern Sweden, The Boston Consulting Group, Technical report. http://www.bcg.se/documents/file164478.pdf
51. Fortum (2016) Open district heating. http://www.opendistrictheating.com/
52. N.R.E.L. (NREL), Energy system integration facility (esif). https://hpc.nrel.gov/datacenter